Top-down Lipidomics of Low Density Lipoprotein reveal altered Lipid Profiles in Advanced Chronic Kidney Disease

[1]Ana Reis (PhD), [2]Alisa Rudnitskaya (PhD), [3$]Pajaree Chariyavilaskul (PhD), [3,4]Neeraj Dhaun (PhD), [3]Vanessa Melville (MSc), [4]Jane Goddard (PhD), [3]David J. Webb (FRCP), [1]Andrew R. Pitt (DPhil), [1*] Corinne M Spickett (DPhil)

[1] School of Life and Health Sciences, Aston University, Birmingham, UK;

[2] CESAM, Department of Chemistry, Universidade de Aveiro, Portugal;

[3] Clinical Pharmacology Unit, BHF Centre of Research Excellence, Queen's Medical Research Institute, University of Edinburgh, Edinburgh, UK;

[4] Department of Renal Medicine, Royal Infirmary of Edinburgh, UK;

[$] Current address: Department of Pharmacology, Faculty of Medicine, Chulalongkorn University, Thailand.

Running title: Lipid profiles in chronic kidney disease

Corresponding Author (*)

Corinne M Spickett, School of Life and Health Sciences, University of Aston, Aston Triangle, Birmingham, B4 7ET, UK. Tel. +44(0)121 2044085

Email: c.m.spickett@aston.ac.uk;

ABSTRACT

This study compared the molecular lipidomic profile of LDL in patients with non-diabetic advanced renal disease and no evidence of cardiovascular disease to that of age-matched controls, with the hypothesis that it would reveal proatherogenic lipid alterations. LDL was isolated from 10 normocholesterolemic patients with stages 4/5 renal disease and 10 controls, and lipids were analysed by accurate mass liquid chromatography-mass spectrometry. Top-down lipidomics analysis and manual examination of the data identified 352 lipid species, and automated comparative analysis demonstrated alterations in lipid profile in disease. The total lipid and cholesterol content was unchanged, but levels of triacylglycerides and N-acyltaurines were significantly increased, while phosphatidylcholines, plasmenyl ethanolamines, sulfatides, ceramides and cholesterol sulfate were significantly decreased in CKD patients. Chemometric analysis of individual lipid species showed very good discrimination of control and disease sample despite the small cohorts, and identified individual unsaturated phospholipids and triglycerides mainly responsible for the discrimination. These findings illustrate the point that although the clinical biochemistry parameters may not appear abnormal, there may be important underlying lipidomic changes that contribute to disease pathology. The lipidomic profile of CKD LDL offers potential for new biomarkers and novel insights into lipid metabolism and cardiovascular risk in this disease.

Keywords

Cholesterol, Dyslipidemias, Inflammation, Phospholipids, Mass spectrometry;

Cholesterol sulfate, N-acyltaurine, Partial least squares discriminant analysis**.**

Introduction

Chronic kidney disease (CKD) is a serious and increasingly common condition (1). Patients with CKD have a greatly increased risk of cardiovascular disease (CVD), which represents the most common cause of mortality and morbidity in these patients, to the extent that CKD is considered an independent risk factor for CVD (2, 3). In CKD, many conventional risk factors for CVD are prevalent, including hypertension, dyslipidemia and insulin resistance. Underlying conditions that are typical of CVD also occur, such as heightened inflammatory status, oxidative stress, endothelial dysfunction and arterial stiffness (3, 4). Consequently, understanding the factors in CKD that could contribute to increased CVD risk is very important.

In CVD there is a clearly established link between dyslipidemia (specifically hypercholesterolemia and hypertriglyceridemia) and atherosclerosis, an underlying pathology of most CVD (5, 6). In view of the clear cardio-renal relationship, there has been considerable interest in the possible contribution of hyperlipidemia to CKD-associated CVD (7, 8). The nature of this lipid imbalance is significantly different to non-renal-related CVD; in particular, the relationship with cholesterol level is less clear than in the general population and is dependent on the stage of disease (9, 10). In some patients, total cholesterol and LDL-cholesterol are not elevated, while patients on hemodialysis may even have reduced cholesterol compared to control subjects (11). It is apparent that CKD involves multiple lipid abnormalities, some of which may contribute to increased CVD risk. However, most studies of lipid abnormalities in CKD have focused on lipoprotein profile or on overall lipid classes such as triglycerides. Whilst in many inflammatory diseases, including pre-eclampsia (12), diabetes (13), rheumatoid arthritis (14) and Crohn's disease (15), lipidomic studies have identified characteristic lipid signatures that have potential as diagnostic tools, there have as yet been few attempts at profiling individual lipids in CKD. Evidence for an altered phospholipid profile in CKD (16) and a decrease of serum sulfatide levels in patients with end-stage renal failure (17) have been reported, but otherwise little is known about molecular changes.

Modern lipidomics depends almost entirely on analysis by electrospray mass spectrometry, as this is able to identify a very wide variety of individual lipid species in several classes. Both shotgun lipidomics, involving direct infusion of the sample into the instrument, and liquid chromatography coupled to mass spectrometry (LC-MS) are widely used for this purpose (18). Chromatographic separation provides additional information to facilitate lipid identification, and separation of the lipids reduces interference (19). Although with lower resolution instruments, tandem MS is necessary to distinguish lipids of similar mass but different formula, modern high resolution instruments such as orbitraps offer sufficient mass accuracy that isobaric species can be distinguished, thus allowing classification of lipid analytes and identification of the total number of carbons and double bonds in the acyl chains by a top-down approach (20). It has been demonstrated that this untargetted approach, coupled with principle component analysis, can be used without internal standards for comparative analysis of lipidomes, owing to the high dynamic range of the orbitrap (21). Similar "semi-quantitative" approaches on a triple quadrupole instrument have also been used for comparative lipidomics in cardiovascular disease (22, 23). However, tandem MS or MS^n is still required for confirmation of individual acyl chain length and double bonds.

We recently demonstrated that a top-down lipidomics approach using liquid chromatography interfaced to mass spectrometry on a high resolution instrument (Orbitrap Exactive) was able to identify more than 350 individual lipid species or isomeric lipid clusters in normo-lipidemic LDL (24). The lipids were identified by matching the experimental *m/z* for the molecular ions to calculated mono-isotopic masses available in lipidomic and metabolic databases. LDL is an important carrier of a wide variety of lipid species within the plasma, and reflects systemic changes in lipid metabolism. We hypothesized that the application of this methodology to CKD would identify novel differences in lipid profile at a molecular level between disease and control samples that would enhance understanding of the disease mechanisms and offer potential as diagnostic markers.

MATERIALS AND METHODS

Materials

All chemicals used were of analytical quality and purchased from Sigma-Aldrich (UK) or ThermoFisher (UK) unless stated otherwise. Organic solvents were HPLC grade purchased from Fisher Scientific (Loughborough, UK).

Subjects and blood collection

Male CKD patients (stage 4/5) were recruited from the renal outpatient clinic at the Royal Infirmary of Edinburgh following ethical approval by NHS Lothian Research Ethics Committee and gave informed consent as described previously (25). Renal patients were excluded on the basis of renal transplant, dialysis, systemic vasculitis or connective tissue disease, a history of established cardiovascular disease, peripheral vascular disease, diabetes mellitus, respiratory disease, neurological disease, alcohol abuse or treatment with an organic nitrate or β-agonist. The causes of kidney disease in patients were autosomal dominant polycystic kidney disease (n=4), IgA nephropathy (n=2), reflux nephropathy (n=3) and neurogenic bladder (n=1). Smokers and hypercholesterolemic patients were not excluded, but the latter were controlled by statin medication (2 individuals in the disease group) and stable on treatment for 3 months prior to inclusion in the study. Subjects refrained from alcohol for at least 24h, and caffeinated drinks and smoking for at least 12 h before the study.

Blood samples were collected in polypropylene tubes containing EDTA (final concentration, 1 mg/mL of blood), plasma was promptly separated by centrifugation (2500xg, 20 min, 4°C) and stored in 2 mL aliquots at -80°C in the dark.

Clinical and biochemical measurements

Blood pressure, hsCRP, OxLDL and IL-6 were determined as described previously (25). Other parameters (plasma glucose, total cholesterol, triglyceride, lipoproteins, creatinine and glycated hemoglobin (HbA_{1c})) were determined in the hospital biochemistry laboratory by assays validated to GLP standard.

Plasma samples and LDL separation

LDL was isolated from plasma aliquots essentially as described previously (26). KBr (0.3816 mg) was dissolved in 1 mL of plasma at 4°C, and underlaid below 4.1 ml of a deoxygenated EDTA solution, before centrifuging in a Beckman VTi 90 rotor for 2 hours at 60,000 rpm to generate a density gradient. LDL formed bands in the density range 1.019-1.060 g/mL. The LDL collected was stored in sterile vials under nitrogen, and desalted before determining the cholesterol content using CHOL PAD reagent (Roche Diagnostics) and protein concentration of isolated LDL was determined by the Bradford assay as reported by Yue et al. (27). Purity of isolated LDL was confirmed by polyacrylamide gel electrophoresis (24, 28).

Vitamin E content

Vitamin E content (α-tocopherol) in LDL was determined by reverse-phase chromatography using spectrophotometric detection as described previously (29). The samples and standards were injected randomly in triplicate and area under the curve (AUC) was plotted against the calibration curves and used to calculate the concentration of vitamin E in the samples (μg/mg protein). Standards (0.1-10 μg/mL), made up in methanol and extracts redissolved in 100 μL methanol, were analysed in triplicate by injection of 20μL. The intraday CV (n=3) at a concentration of 2.5 μg/mL was 3.1%. Statistical analysis was carried out using an unpaired *t* test, with Welch's correction to estimate the *p* values.

Electrophoretic mobility of LDL

The particle size of LDL was assessed by 1% agarose gel electrophoresis in barbital buffer as described previously (30). Retardation factors (Rf) were defined as the distance (cm) travelled by sample / distance (cm) travelled by dye front.

Lipid Extraction

LDL lipids were extracted from LDL containing 25 μg protein by the Folch method as described recently (24). The lipid extracts were combined into an amber vial (Supelco), dried

under a stream of nitrogen filtered with a 0.22 µm mesh (Millipore) and stored at -70°C until further analysis. Mean recovery (%) of PC (13:0/13:0) lipid standard in spiked LDL samples by the Folch method was 103.9±8.6. Similar recoveries were achieved with dehydroepiandrosterone sulfate as a representative of more polar lipid classes, and d5-myristic acid (Sigma Aldrich Chemical Co, UK) as a representative of less polar lipids.

Top-down LC-MS analysis of lipidomic profile

Lipid extracts were solubilized in 100 µL $CHCl_3$:MeOH (1:1, v/v), further diluted in MeOH and analysed by LC-MS essentially as described previously (24). Separation of LDL lipid classes was performed using a Dionex Ultimate 3000 HPLC system (Thermo Scientific, Hemel Hempstead) by injection of 10 µL sample onto a silica gel column (150mm x 3mm x 3µm, HiChrom, Reading, UK) used in hydrophilic interaction chromatography (HILIC) mode (24). Two solvents were used: (A) 20% isopropyl alcohol (IPA) in acetonitrile and (B) 20% IPA in ammonium formate (20 mM). Elution was achieved using the following gradient at 0.3 mL/min: elution at 5% B for 1 min, followed by a rise to 9% B at 5 min, to 15% B at 10 min, to 25% B at 16 min, to 35% B at 23 min, and from 28-40 min a decrease to 5% B. Detection of lipids was performed in a Orbitrap Exactive Mass Spectrometer (ThermoFisher Scientific Inc., Bremen, Germany) equipped with polarity switching. The instrument was calibrated according to the manufacturer specifications to give an rms mass error <2 ppm. The following electrospray ionization settings were used: source voltage: ±4.50 kV, capillary voltage: 25 V, capillary temp: 320^{o}C, sheath gas flow: 50 AU, aux gas flow: 17 AU, sweep gas flow: 0 AU. All LC-MS spectra were recorded in the *m/z* range 100-1200 at 50,000 resolution (FWHM at *m/z* =500). Three microscans were collected per data point with the injection time limited by either an automatic gain control target ion intensity of 10^6 or a maximum inject time of 250 ms.

For certain lipids of interest, tandem mass spectrometry (MS^2) was carried out on an LTQ Orbitrap instrument (ThermoElectron, Hemel Hempstead, UK) controlled by Xcalibur (version 2.0, Thermo Fisher Corporation) in either positive or negative ion modes as appropriate for the

best detection of the parent ion. The capillary voltage was set at 4.5kV, capillary temperature at 275°C, with sheath gas and sweep gas flow rates set at 30 and 10 AU respectively. Collision energy was set according to the ion of interest, typically between 25-35 (arbitrary units).

LC-MS data processing

In the first stage, LC-MS data were analysed and lipid species identified by manual matching of retention times and accurate mass data to a home-built database and the Human Metabolome project database (HMDB) (31), with identifications based on ions showing a mass error of <5 ppm (and in most cases <2 ppm) to the mono-isotopic mass calculated from the theoretical formula. 352 lipids were identified by this approach.

Subsequently, LC-MS data were analysed by filtering with MZMatch (32) followed by using the XCMS pipeline (XCMS Online version 0.0.83, Scripps Center for Metabolomics, https://xcmsonline.scripps.edu/, (33)) for peak detection, alignment and isotope annotation as described previously (24). Ions with intensity <5000 cps were excluded. Integration of features extracted in different samples corresponds to the reported extracted ion chromatogram areas. Peak intensities for the ions identified from individual lipid classes in the datasets were summed and used to evaluate overall differences in disease vs. age-matched control groups. Extracted features were included if they were present in >50% of the samples in each group, were within 2.5 ppm from the exact mono-isotopic mass, and with < 5s retention time deviation. In order to prevent overestimation of the number of lipid species identified, all lipid species detected in positive and negative ion modes were manually cross-referenced. Overall, 142 and 158 individual lipids were identified in positive and negative ion modes, respectively. Isomeric species are reported as one single ion, for instance PC(16:0/18:1), PC(18:1/16:0), PC(16:1/18:0), PC(18:0/16:1), PC(14:0/20:1) and others are expressed as PC(34:1). The data processing steps and number of features or lipids identified at each stage are summarized in Supplementary Figure 1.

Statistical analysis

The merged data set comprising 300 lipids species (Supplementary Figure 1), were further analysed using Partial Least Squares Discriminant Analysis (PLSDA) (34, 35). PLSDA calibration models were validated using segmented cross-validation, and optimization of PLSDA models was achieved using the Variable Importance in Projection (VIP) score (36). A VIP cut-off value of 0.8 was repeatedly applied to eliminate less discriminating variables, with a cut-off of 0.85 for the merged set. The final classification model included 48 species detected in the positive mode and 55 in the negative mode. The statistical significance of the classification PLSDA models was assessed using permutation testing with 1000 permutations (37). Q^2 was used as quality-of-fit criterion for the permutation test (38). Further details are given in Supplemental methods.

Statistical analysis of clinical and biochemical parameters was conducted using non-parametric *t*-tests (Mann-Whitney) using two-tailed p value calculation, and values with $p<0.05$ were considered statistically significant.

RESULTS

Evaluation of clinical and biochemical parameters in kidney disease

Baseline measurements of clinical and biochemical parameters for age- and body mass-matched subjects included in this study are summarized in Table 1. Glomerular filtration rate (GFR) was estimated using the MDRD equation and confirmed all patients as stage 4 or 5 CKD; they also had significantly increased systolic BP. There were no significant differences in levels of glycated hemoglobin and plasma glucose. The inflammatory marker C-reactive protein was significantly elevated, although IL-6 was not. The levels of total plasma cholesterol and LDL were not altered with CKD and there was no change in OxLDL. In contrast, HDL levels showed a significant decrease and plasma triglycerides were elevated, as expected for patients with CKD and published previously (25). LDL vitamin E content and particle heterogeneity (electrophoretic mobility) were also determined but there was no statistical difference (Table 1).

Analysis of LDL from control and CKD samples by manual matching to databases identified more than 300 different lipid species

In order to investigate the lipidome of LDL from control and CKD patients, LDL extracts were analysed by normal-phase liquid chromatography mass spectrometry (LC-MS) in both positive and negative ion modes as reported previously (24). Representative chromatograms for control and CKD samples in each mode are shown in Figure 1. The various chromatographic peaks observed correspond to the elution of different lipid classes. Some lipid species were observed in both positive and negative ionization modes, as indicated by the appearance of peaks with the same retention times, notably in the retention time ranges 2-3.5 and 20.5-22.5 mins. It can be seen that there were no gross changes in the profile of either positively or negatively charged lipids between sample types, although some minor changes in intensity of chromatographic peaks eluting with retention times shorter than 5 mins were apparent.

All features (ions) detected in the chromatograms using XCMS software were recorded by retention times, accurate mass/charge measurement and intensity, to generate a combined list of 1619 distinct features. Manual matching of the experimental values with theoretical databases was carried out to identify lipid species, as well as manual cross-checking for multiple adducted forms of some lipids (e.g. $[MH]^+$, $[MNa]^+$ or $[M+NH_4]^+$ in positive ion mode; $[M-H]^-$ and $[M+HCOO]^-$ in negative ion mode) to avoid duplication, and isomeric species are reported as one single ion. A summary list corresponding to 352 individual lipid and lipid-related species covering 18 lipid classes or subclasses was compiled (Table 2), which were very similar to those reported previously in healthy volunteers (24). The full list of lipid species detected is given in Supplemental Table 1.

Comparative analysis showed changes in CKD LDL lipid classes including cholesterol sulfate, sulfatides, ceramides and lysolipid ratios

In order to investigate the hypothesis that changes in molecular composition of LDL occur in CKD, an automated analysis of the LC-MS data using the XCMS and MZMatch platform was undertaken. This procedure identified 300 lipid features, 142 in positive ion and 158 in negative ion, which after manual cross-checking for remove adducts and duplicates corresponded to approximately two thirds of the lipid species identified by manual analysis. The smaller number of positive identifications results from several factors, including the exclusion of ions with intensity <5000 cps, the requirement that peaks were present in >50% of samples in either group, and the ability of the programme to adjust for minor differences in retention times.

The intensities of ions identified in this dataset were summed to provide an estimate of the total lipid intensity and the lipid intensity in each of the identified classes, following a previously published procedure (24). The variability of total lipids extracted (extraction repeatability and analytical reproducibility) between replicates in the samples of control and disease group was <10%, thus enabling this approach to be used for comparisons of lipid content

between samples for any one lipid class, although it cannot be used for comparisons between lipid classes owing to differences in ionization efficiencies.

The total lipid in LDL remained essentially unaltered in the CKD patient group compared to the age-matched control group (Figure 2a), but changes in the intensity of a number of lipid classes were observed in LDL. There was an observed statistically significant increase in triacylglycerides (Figure 2b), in agreement with the clinical data in Table 1, whereas the content of phosphatidylcholines decreased significantly in the CKD group (Figure 2c). There were no changes in the intensities of total cholesterol and sphingomyelins, or in the total levels of phosphatidylethanolamines (PE) (data not shown), although the contribution of PE containing a vinyl ether linkage to the total PE pool was significantly lower in CKD samples (Figure 2d). Interestingly, the total content of lyso-lipids (LPC+LPE) in LDL in disease patients was similar when compared to age-matched controls (Figure 2e), but the ratio of lyso-lipid types (LPC/LPE) showed a significant decrease in LDL from CKD samples (Figure 2f). In addition, changes in CKD were observed in 4 other lipid class that constitute minor components of LDL; specifically, the content of ceramides (Figure 3a), cholesterol sulphate (Figure 3b) and sulfatides (Figure 3c) decreased significantly in LDL from CKD patients, whereas a significant increase was observed in the content of N-acyltaurines(Figure 3d). Thus in addition to changes in commonly assessed lipid class triglycerides, CKD patients show changes in both abundant and minor lipid components of LDL that are not apparent simply from standard lipoprotein assessment.

Statistical analysis discriminated control and CKD LDL lipidomes based on individual species of unsaturated phospholipids and triglycerides.

For a full statistical analysis of the MS data and to identify the contribution of individual lipid species to differences between the control and CKD samples, Partial Least Squares Discriminant Analysis (PLSDA) was used. The classification summary for three optimized models calculated using lipid profiles measured in positive and negative ion modes and the

merged (+ve plus –ve mode) data set, are shown in Table 3. Q^2 values, which are a measure of the ability of the model to predict correctly the class, lie between 0.79 and 0.82. Values of 0.5 are often classed as acceptable, and 0.8 as good, for PLSDA analysis of datasets with a limited number of classes. The power of the discrimination is further illustrated by the PLSDA score plot for the merged data (Figure 4), which shows the samples from control and CKD cluster together, and that the classes are well separated from each other within the plot. Similar statistical results were obtained for all three data sets, with a correct classification rate (percentage of samples assigned to the correct class) between 94% and 98%, sensitivity (true positive rate, a measure of the proportion of positive correctly assigned) between 0.93 and 0.97, and specificity (true negative rate, a measure of the proportion of negatives correctly assigned) between 0.96 and 1 for the cross-validation data, though slightly better results were obtained using merged data (Table 3). The closer the values are to 1 the better the quality of the model. The ions that contributed most strongly to the discrimination can be determined from their contribution to the PLSDA model, and were unsaturated lipid species from the most abundant lipid classes, namely PC, TAG and PE; the complete set of discriminating ions is indicated in Supplemental Table 2. Comparison of PLSDA score and loading plots obtained using the merged (+ve plus –ve mode) data set shows that higher levels of lipid species from the PE class and some species from TAG and SM classes are present in the samples from the disease group, while all other lipid species are present at lower concentration. Two examples of the lipids that contributed strongly to the lipidomic alteration in LDL from CKD patients include plasmenyl PC 40:7 at *m/z* 818.6060 (Figure 5a, decreased in CKD) and plasmenyl PE 38:7 at *m/z* 746.5137 (Figure 5b, decreased in CKD).

Discussion

CKD is associated with increased risk of CVD and dyslipidemia contributes to this increased risk (2-4), but until recently studies of lipids in CKD have mainly focused on lipoprotein balance or measured total levels of major classes (7, 11, 39). To test the hypothesis that molecular information about LDL lipidomic profile would reveal novel details of dyslipidemia in CKD, we used a top-down lipidomic approach that allows a comparative analysis (20, 22, 23) of the LDL lipid profile from age-matched controls and patients with stage 4/5 CKD. This identified significant differences in LDL lipidome of CKD patients. Multivariant analysis by PLSDA showed very good discrimination of the control and disease data sets, with a combination of positively and negatively charged lipids providing the best discrimination. The lipid species that contributed most were specific isomeric clusters from the abundant lipid classes, namely phosphatidylcholines (decreased), triglycerides (increased) and plasmenylethanolamines (decreased as a proportion of total PE), as these contain a large number of individual lipids, many of which are known to be present at relatively high levels in LDL (40). However, minor lipid subclasses also showed significant differences in CKD and control LDL, specifically cholesterol sulphate, sulfatides, and ceramides, which were lower in CKD LDL, and N-acyltaurines, which increased in CKD LDL, compared to control. Thus although the clinical lipoprotein profile only showed an increase in triglycerides and a decrease in HDL, detailed molecular analysis identified several lipid classes and subclasses that are altered in LDL, and within these classes, changes in several molecular lipid species.

Some of the molecular changes observed in the LDL lipidome in CKD are linked to atherogenic mechanisms, and therefore could explain the increased risk of CVD in these patients. PCs are phospholipids present in the surface monolayer of LDL, and are important for the conformation of ApoB-100, macrostructure of LDL, and its correct interaction with LDL receptors (41, 42). Interestingly, the overall decreased PC observed in this study was apparently not sufficient to cause major structural changes in the LDL, as there was no significant change in

the size of the LDL particles in CKD. The decrease in PCs observed is in agreement with a previous report on levels of PC in plasma of end stage renal failure (ESRF) patients (43), and also with the observation that PCs are lost in urine of patients with CKD (44). The lower levels of sulfatides and cholesterol sulfates in LDL of CKD patients are in agreement with some previous studies (17). Sulfatides are anionic glycosphingolipids that are known to have anti-thrombotic effects, although opposing effects have also been reported under certain experimental conditions (17, 45). Within LDL, they confer negative charge at the particle surface and have been suggested to act as endogenous ligands for chemokines (46) and some selectins (47). Thus it is clear that they have complex effects within the cardiovascular system and decreased levels could upset delicately balanced processes such as thrombosis and LDL-endothelial cell interactions. Hu et al. (17) reported that sulfatides were the only factor that discriminated control from ESRF groups in their study, and that they have promise as biomarkers for CKD. We observed a decrease in the level of ceramides in LDL from CKD patients; however, as increased sphingomyelinase activity and free ceramides are thought to be linked to atherogenesis (48, 49), this does not appear to contribute to the pro-atherogenic profile of CKD. Finally, it was also noted that there was a significant increase in taurine-containing lipoamino acids (LAA) in LDL from CKD patients. LAAs are well known as components of mammalian nervous tissue and are involved in signaling neuronal events (50), and have only recently been detected in LDL (24). In neuronal ischemia these lipids have been reported to show protective and anti-inflammatory effects (51), but they can also induce apoptosis of macrophages (52). As yet, their role in lipoproteins and potential atherogenic contribution has not been elucidated.

A limitation of this study is that only patients with severe kidney disease and age-matched controls were compared, so, in the absence of intermediate stages, limited conclusions about the role of these changes in disease progression can be drawn. Also, the CKD patients studied here had minimal comorbidity with no current clinically apparent CVD, despite the high risk of developing CVD. Although in this cohort the levels of hsCRP were high, indicating some

inflammation, IL-6 and measures of oxidative stress (OxLDL) were low. These findings differ from some previous studies (3, 4) where both inflammation and oxidative stress were substantially increased in CKD and contribute significantly to its accelerated vascular pathology. Our data suggest that uremia is not itself pro-oxidant and this feature may be driven largely by co-morbidity. However, it is unclear whether uremia or increased inflammation are responsible for the LDL lipidomic changes, or result from them. These changes in CKD patients are unlikely to be the consequence of lipid lowering drugs, as only 2 patients were on statin therapy and none was on fibrate therapy. A full understanding of the role of LDL lipidomics in CVD risk in CKD patients would require a prospective study with comparison of intermediate stages of CKD, as well as CKD with and without CVD complications.

A limitation of the top-down lipidomic methodology is that some features in the mass spectra remain unidentified and it is not possible to discriminate some individual lipids within isomeric clusters, so further differences could be present that are not reported here. It should be noted that as internal standards were not used, the analysis is comparative and semi-quantitative. Such approaches have been reported previously (21-23) and have the advantage of avoiding the high expense of labeled compounds, although they do not allow the fully quantitative analysis that can be achieved with use of isotope-labeled internal standards (53). Finally, although, bootstrapping of the test data gave very good sensitivity and selectivity for discrimination, demonstrating the robustness of the analysis, further analysis on a validation data set would be desirable as the next stage of study.

In summary, using an LC-MS approach we report the first comprehensive top-down lipidomic signature of LDL in kidney disease patients with normocholesterolemia. Patients with stage 4/5 CKD demonstrated significant changes in the lipidome of their LDL compared to age-matched controls, and multivariant analysis gave very good discrimination of control and disease samples, despite the small cohorts used (n=10). These findings illustrate the point that although the clinical biochemistry parameters may not appear abnormal, there may be important

underlying lipidomic changes that contribute to disease pathology. The lipidomic profile of CKD LDL offers potential for new biomarkers and novel insights into lipid metabolism and cardiovascular risk in this disease. Further work with early disease stages is now warranted to enable the relationship of these lipids with disease severity and cardiovascular events to be correlated.

Abbreviations

CKD, chronic kidney disease; CVD, cardiovascular disease; dPC, diacyl phosphatidylcholine (ester linkages);dPE, diacyl phosphatidylethanolamine (ester linkages); ESRF, end stage renal failure; GFR, glomerular filtration rate; LC-ESI-MS, liquid chromatography electrospray ionization mass spectrometry; LPC, lyso-phosphatidylcholine; LPE, lyso-phosphatidylethanolamine; NAT, N-acyltaurines; OxLDL, oxidized LDL; PC, phosphatidylcholine; pPC, plasmanyl/plasmenyl cholines; PE, phosphatidylethanolamine; pPE, plasmanyl/plasmenyl ethanolamines; PLSDA, Partial Least Squares Discriminant Analysis; SM, sphingomyelin; TAG, triacylglycerol / triglycerides.

Acknowledgements

Sources of funding **–** This research was supported by a Marie Curie Intra-European Fellowship within the 7th European Community Framework Program (IEF 255076). Work of A. Rudnitskaya was supported by the Portuguese Science and Technology Foundation, through the European Social Fund (ESF) and "Programa Operacional Potencial Humano – POPH. We would like to thank Mr. David Hardy for performing the vitamin E analysis. The clinical study from which the lipidomic data were extracted was funded by a British Heart Foundation project grant (PG/05/91). Dr Lilitkarntakul was supported by the Royal Thai Government. ND is supported by a British Heart Foundation Intermediate Clinical Research Fellowship (FS/13/30/29994).

Disclosures – None of the authors have relationships with any companies that would have a financial interest in the information contained in the manuscript.

References

1. Meguid El Nahas, A., and A. K. Bello. 2005. Chronic kidney disease: the global challenge. *Lancet* **365**: 331-340.

2. Sarnak, M. J., A. S. Levey, A. C. Schoolwerth, J. Coresh, B. Culleton, L. L. Hamm, P. A. McCullough, B. L. Kasiske, E. Kelepouris, M. J. Klag, P. Parfrey, M. Pfeffer, L. Raij, D. J. Spinosa, and P. W. Wilson. 2003. Kidney disease as a risk factor for development of cardiovascular disease - A statement from the American Heart Association councils on kidney in cardiovascular disease, high blood pressure research, clinical cardiology, and epidemiology and prevention. *Circulation* **108**: 2154-2169.

3. Schiffrin, E. L., M. L. Lipman, and J. F. E. Mann. 2007. Chronic kidney disease - Effects on the cardiovascular system. *Circulation* **116**: 85-97.

4. Zoccali, C. 2006. Traditional and emerging cardiovascular and renal risk factors: An epidemiologic perspective. *Kidney Int* **70**: 26-33.

5. Steinberg, D. 2005. Hypercholesterolemia and inflammation in atherogenesis: Two sides of the same coin. *Mol Nutr Food Res* **49**: 995-998.

6. Shepherd, J. 2004. Lipids in health and disease. *Biochem Soc Trans* **32**: 1051-1056.

7. Keane, W. F., J. E. Tomassini, and D. R. Neff. 2013. Lipid Abnormalities in Patients with Chronic Kidney Disease: Implications for the Pathophysiology of Atherosclerosis. *J Atheroscler Thromb* **20**: 123-133.

8. Cheung, A. K. 2009. Is Lipid Control Necessary in Hemodialysis Patients? *Clin J Am Soc Nephrol* **4**: S95-S101.

9. Kaysen, G. A. 2009. Lipid and Lipoprotein Metabolism in Chronic Kidney Disease. *J Ren Nutr* **19**: 73-77.

10. Vaziri, N. D., and K. Norris. 2011. Lipid Disorders and Their Relevance to Outcomes in Chronic Kidney Disease. *Blood Purif* **31**: 189-196.

11. Lacquaniti, A., D. Bolignano, V. Donato, C. Bono, M. R. Fazio, and M. Buemi. 2010. Alterations of Lipid Metabolism in Chronic Nephropathies: Mechanisms, Diagnosis and Treatment. *Kidney Blood Press Res* **33**: 100-110.

12. Romanowicz, L., and E. Bankowski. 2010. Sphingolipids of human umbilical cord vein and their alteration in preeclampsia. *Mol Cell Biochem* **340**: 81-89.

13. Barber, M. N., S. Risis, C. Yang, P. J. Meikle, M. Staples, M. A. Febbraio, and C. R. Bruce. 2012. Plasma lysophosphatidylcholine levels are reduced in obesity and type 2 diabetes. *PLoS One* **7**: e41456.

14. Giera, M., A. Ioan-Facsinay, R. Toes, F. Gao, J. Dalli, A. M. Deelder, C. N. Serhan, and O. A. Mayboroda. 2012. Lipid and lipid mediator profiling of human synovial fluid in rheumatoid arthritis patients by means of LC-MS/MS. *Bba-Biomembranes* **1821**: 1415-1424.

15. Sewell, G. W., Y. A. Hannun, X. Han, G. Koster, J. Bielawski, V. Goss, P. J. Smith, F. Z. Rahman, R. Vega, S. L. Bloom, A. P. Walker, A. D. Postle, and A. W. Segal. 2012. Lipidomic profiling in Crohn's disease: abnormalities in phosphatidylinositols, with preservation of ceramide, phosphatidylcholine and phosphatidylserine composition. *Int J Biochem Cell Biol* **44**: 1839-1846.

16. Jia, L. W., C. Wang, S. M. Zhao, X. Lu, and G. W. Xu. 2007. Metabolomic identification of potential phospholipid biomarkers for chronic glomerulonephritis by using high performance liquid chromatography-mass spectrometry. *J Chromatogr B Analyt Technol Biomed Life Sci* **860**: 134-140.

17. Hu, R., G. Li, Y. Kamijo, T. Aoyama, T. Nakajima, T. Inoue, K. Node, R. Kannagi, M. Kyogashima, and A. Hara. 2007. Serum sulfatides as a novel biomarker for cardiovascular disease in patients with end-stage renal failure. *Glycoconjugate J* **24**: 565-571.

18. Han, X. L., K. Yang, and R. W. Gross. 2012. Multi-dimensional mass spectrometry-based shotgun lipidomics and novel strategies for lipidomic analyses. *Mass Spectrom Rev* **31**: 134-178.

19. Lam, S. M., and G. H. Shui. 2013. Lipidomics as a Principal Tool for Advancing Biomedical Research. *Journal of Genetics and Genomics* **40**: 375-390.

20. Schwudke, D., K. Schuhmann, R. Herzog, S. R. Bornstein, and A. Shevchenko. 2011. Shotgun Lipidomics on High Resolution Mass Spectrometers. *Csh Perspect Biol* **3**.

21. Schwudke, D., J. T. Hannich, V. Surendranath, V. Grimard, T. Moehring, L. Burton, T. Kurzchalia, and A. Shevchenko. 2007. Top-down lipidomic screens by multivariate analysis of high-resolution survey mass spectra. *Anal Chem* **79**: 4083-4093.

22. Stegemann, C., I. Drozdov, J. Shalhoub, J. Humphries, C. Ladroue, A. Didangelos, M. Baumert, M. Allen, A. H. Davies, C. Monaco, A. Smith, Q. Xu, and M. Mayr. 2011. Comparative lipidomics profiling of human atherosclerotic plaques. *Circ Cardiovasc Genet* **4**: 232-242.

23. Stegemann, C., R. Pechlaner, P. Willeit, S. R. Langley, M. Mangino, U. Mayr, C. Menni, A. Moayyeri, P. Santer, G. Rungger, T. D. Spector, J. Willeit, S. Kiechl, and M. Mayr. 2014. Lipidomics profiling and risk of cardiovascular disease in the prospective population-based Bruneck study. *Circulation* **129**: 1821-1831.

24. Reis, A., A. Rudnitskaya, G. J. Blackburn, N. M. Fauzi, A. R. Pitt, and C. M. Spickett. 2013. A comparison of five lipid extraction solvent systems for lipidomic studies of human LDL. *J Lipid Res* **54**: 1812-1824.

25. Lilitkarntakul, P., N. Dhaun, V. Melville, S. Blackwell, D. K. Talwar, B. Liebman, T. Asai, J. Pollock, J. Goddard, and D. J. Webb. 2011. Blood pressure and not uraemia is the major determinant of arterial stiffness and endothelial dysfunction in patients with chronic kidney disease and minimal co-morbidity. *Atherosclerosis* **216**: 217-225.

26. Jerlich, A., A. R. Pitt, R. J. Schaur, and C. M. Spickett. 2000. Pathways of phospholipid oxidation by HOCl in human LDL detected by LC-MS. *Free Radic Biol Med* **28**: 673-682.

27. Yue, H., S. A. Jansen, K. I. Strauss, M. R. Borenstein, M. F. Barbe, L. J. Rossi, and E. Murphy. 2007. A liquid chromatography/mass spectrometric method for simultaneous analysis

of arachidonic acid and its endogenous eicosanoid metabolites prostaglandins, dihydroxyeicosatrienoic acids, hydroxyeicosatetraenoic acids, and epoxyeicosatrienoic acids in rat brain tissue. *J Pharm Biomed Anal* **43**: 1122-1134.

28. Mahley, R. W., T. L. Innerarity, S. C. Rall, Jr., and K. H. Weisgraber. 1984. Plasma lipoproteins: apolipoprotein structure and function. *J Lipid Res* **25**: 1277-1294.

29. Zhao, B., S. Y. Tham, J. Lu, M. H. Lai, L. K. Lee, and S. M. Moochhala. 2004. Simultaneous determination of vitamins C, E and beta-carotene in human plasma by high-performance liquid chromatography with photodiode-array detection. *J Pharm Pharm Sci* **7**: 200-204.

30. Aldred, S., and H. R. Griffiths. 2004. Oxidation of protein in human low-density lipoprotein exposed to peroxyl radicals facilitates uptake by monocytes; protection by antioxidants in vitro. *Environ Toxicol Pharmacol* **15**: 111-117.

31. Wishart, D. S., C. Knox, A. C. Guo, R. Eisner, N. Young, B. Gautam, D. D. Hau, N. Psychogios, E. Dong, S. Bouatra, R. Mandal, I. Sinelnikov, J. Xia, L. Jia, J. A. Cruz, E. Lim, C. A. Sobsey, S. Shrivastava, P. Huang, P. Liu, L. Fang, J. Peng, R. Fradette, D. Cheng, D. Tzur, M. Clements, A. Lewis, A. De Souza, A. Zuniga, M. Dawe, Y. Xiong, D. Clive, R. Greiner, A. Nazyrova, R. Shaykhutdinov, L. Li, H. J. Vogel, and I. Forsythe. 2009. HMDB: a knowledgebase for the human metabolome. *Nucleic Acids Res* **37**: D603-610.

32. Scheltema, R. A., A. Jankevics, R. C. Jansen, M. A. Swertz, and R. Breitling. 2011. PeakML/mzMatch: a file format, Java library, R library, and tool-chain for mass spectrometry data analysis. *Anal Chem* **83**: 2786-2793.

33. Tautenhahn, R., G. J. Patti, D. Rinehart, and G. Siuzdak. 2012. XCMS Online: a web-based platform to process untargeted metabolomic data. *Anal Chem* **84**: 5035-5039.

34. Wold, S., M. Sjostrom, and L. Eriksson. 2001. PLS-regression: a basic tool of chemometrics. *Chemom Intell Lab Syst* **58**: 109-130.

35. Barker, M., and W. Rayens. 2003. Partial least squares for discrimination. *J Chemometrics* **17**: 166-173.

36. Chi-Hyuck, J., S. H. Lee, H. S. Park, and J. H. Lee. 2009. Use of partial least squares regression for variable selection and quality prediction. *In* Computers & Industrial Engineering, 2009. CIE 2009. International Conference on Computers & Industrial Engineering, University of Technology of Troyes. 1302-1307.

37. Westerhuis, J. A., H. C. J. Hoefsloot, S. Smit, D. J. Vis, A. K. Smilde, E. J. J. van Velzen, J. P. M. van Duijnhoven, and F. A. van Dorsten. 2008. Assessment of PLSDA cross validation. *Metabolomics* **4**: 81-89.

38. Westerhuis, J. A., E. J. J. Velzen, H. C. J. Hoefsloot, and A. K. Smilde. 2008. Discriminant Q2 (DQ2) for improved discrimination in PLSDA models. *Metabolomics* **4**: 293-296.

39. Keane, W. F., J. E. Tomassini, and D. R. Neff. 2011. Lipid Abnormalities in Patients with Chronic Kidney Disease. *Hemodialysis: New Methods and Future Technology. Contrib Nephrol.* **171**: 135-142.

40. Dashti, M., W. Kulik, F. Hoek, E. C. Veerman, M. P. Peppelenbosch, and F. Rezaee. 2011. A Phospholipidomic Analysis of All Defined Human Plasma Lipoproteins. *Sci Rep-Uk* **1**.

41. Flood, C., M. Gustafsson, R. E. Pitas, L. Arnaboldi, R. L. Walzem, and J. Boren. 2004. Molecular mechanism for changes in proteoglycan binding on compositional changes of the core and the surface of low-density lipoprotein-containing human apolipoprotein B100. *Arterioscler Thromb Vasc Biol* **24**: 564-570.

42. Terpstra, V., D. A. Bird, and D. Steinberg. 1998. Evidence that the lipid moiety of oxidized low density lipoprotein plays a role in its interaction with macrophage receptors. *Proc Natl Acad Sci U S A* **95**: 1806-1811.

43. Piperi, C., C. Kalofoutis, M. Tzivras, T. Troupis, A. Skenderis, and A. Kalofoutis. 2004. Effects of hemodialysis on serum lipids and phospholipids of end-stage renal failure patients. *Mol Cell Biochem* **265**: 57-61.

44. Yang, W. L., Q. Bai, D. D. Li, T. L. A, S. Wang, R. S. Zhao, H. G. Nie, A. H. Zhang, T. Wang, and M. H. Fan. 2013. Changes of urinary phospholipids in the chronic kidney disease patients. *Biomarkers*.

45. Kyogashima, M. 2004. The role of sulfatide in thrombogenesis and haemostasis. *Arch Biochem Biophys* **426**: 157-162.

46. Sandhoff, R., H. Grieshaber, R. Djafarzadeh, T. P. Sijmonsma, A. E. I. Proudfoot, T. M. Handel, H. Wiegandt, P. J. Nelson, and H. J. Grone. 2005. Chemokines bind to sulfatides as revealed by surface plasmon resonance. *Bba-Biomembranes* **1687**: 52-63.

47. Blann, A. D., S. K. Nadar, and G. Y. Lip. 2003. The adhesion molecule P-selectin and cardiovascular disease. *Eur Heart J* **24**: 2166-2179.

48. Kobayashi, K., E. Nagata, K. Sasaki, M. Harada-Shiba, S. Kojo, and H. Kikuzaki. 2013. Increase in secretory sphingomyelinase activity and specific ceramides in the aorta of apolipoprotein E knockout mice during aging. *Biol Pharm Bull* **36**: 1192-1196.

49. Sneck, M., S. D. Nguyen, T. Pihlajamaa, G. Yohannes, M. L. Riekkola, R. Milne, P. T. Kovanen, and K. Oorni. 2012. Conformational changes of apoB-100 in SMase-modified LDL mediate formation of large aggregates at acidic pH. *J Lipid Res* **53**: 1832-1839.

50. Tan, B., D. K. O'Dell, Y. W. Yu, M. F. Monn, H. V. Hughes, S. Burstein, and J. M. Walker. 2010. Identification of endogenous acyl amino acids based on a targeted lipidomics approach. *J Lipid Res* **51**: 112-119.

51. Yao, L. Y., Q. Lin, Y. Y. Niu, K. M. Deng, J. H. Zhang, and Y. Lu. 2009. Synthesis of Lipoamino acids and their activity against cerebral ischemic injury. *Molecules* **14**: 4051-4064.

52. Takenouchi, R., K. Inoue, Y. Kambe, and A. Miyata. 2012. N-arachidonoyl glycine induces macrophage apoptosis via GPR18. *Biochem Biophys Res Commun* **418**: 366-371.

53. Brown, J. M., and S. L. Hazen. 2014. Seeking a unique lipid signature predicting cardiovascular disease risk. *Circulation* **129**: 1799-1803.

Figure Legends

Figure 1. Typical normal-phase LC-MS chromatograms of normolipidemic LDL lipid extract (Control, top) and LDL extract from CKD patients (Disease, bottom) in positive (+ve, left) and negative (-ve, right) ion mode. Lipid extracts were prepared according to the Folch method and chromatograms were normalized to relative intensity (%). Labelled peaks are triacylglycerides and cholesteryl esters (TAG+CE), phosphatidylinositols (PI), phosphatidylethanolamines (PE), phosphatidylcholines (PC) and sphingomyelins (SM). The insets depict a zoomed region for the elution of cholesterol sulphate (CS), N-acyltaurines (NAT), ceramides (Cer) and fatty acids (FA) in negative ion mode.

Figure 2. Box plots showing changes in major lipids in the disease group (n=10) against the age-matched control group (n=10). Samples were analysed in triplicate (n=3) and statistical analysis was carried out using the Mann-Whitney test to estimate the P values. Differences were considered statistically significant at $p<0.05$. Plots are a) total lipids detected; b) triacylglycerides; c) total phosphatidylcholine; d) ratio of plasmenyl ethanolamine to total phosphatidyl-ethanolamine; e) total lyso-phosphatidylcholine and lyso-phosphatidylethanolamine; f) ratio of lyso-phosphatidylcholine to lyso-phosphatidylethanolamine.

Figure 3. Box plots of minor lipids that showed significant change in disease. Samples from the disease group (n=10) and the age-matched control group (n=10) were analysed in triplicate and statistical analysis was carried out using the Mann-Whitney test to estimate the p values. Differences were considered statistically significant at $p<0.05$. The plots are a) ceramides; b) N-acyltaurines; c) cholesteryl sulphate; d) sulfatides.

Figure 4. PLSDA scores plot for merged data (lipids detected in positive and negative ion mode). Numbers adjacent to the symbols are patient sample codes.

Figure 5. Boxplots of 2 individual lipid species that were altered in positive (PC) and negative ion mode (PE). Samples from the CKD group (n=10) and age-matched control group (n=10) were analysed in triplicate and statistical analysis was carried out using the Mann-Whitney test to estimate the p values. Differences were considered statistically significant at $p<0.05$. Plots are a) plasmenyl PC 40:7 and b) plasmenyl PE 38:7, where the numbers (C:n) correspond to the total number of carbon atoms: number of double bonds present in the acyl and alkyl chains (including the vinyl ether bond).

Table 1. Clinical biochemistry parameters in plasma for control subjects and chronic kidney disease patients.

Clinical parameters	Controls	CKD*	p-value
n	10	10	-
Age (years)	47±6	44±3	0.111
BMI (kg/m^2)	26±2	29±6	0.113
Smokers/ex-smokers/non-smokers	0/1/9	2/2/8	-
Systolic Blood Pressure (mm Hg)	113±12	124±10	**0.049**
Diastolic Blood Pressure (mm Hg)	72±11	78±6	0.103
Mean Arterial Pressure (mm Hg)	85±11	93±7	0.065
Pulse Pressure (mm Hg)	42±6	46±7	0.189
Plasma Glucose (mg/dL)	5.1±0.5	4.8±0.4	0.231
HbA_{1c} (% of Hb)	5.3±0.40	5.6±0.50	0.117
Serum creatinine (mg/dL)	85±11	460±179	**<0.0001**
MDRD eGFR (mL/min/1.73 m^2)	91.2±14.1	14.8±5.3	**<0.0001**
High sensitivity C-reactive protein (µg/mL)	1.2±1.5	4.2±3.5	**0.027**
IL-6 (pg/mL)	9.6±10.5	7.9±8.7	0.713
Total Cholesterol (mg/dL)	5.1±0.8	4.5±0.8	0.130
Triglycerides (mmol/L)	1.0±0.3	1.8±0.7	**0.004**
HDL (mmol/L)	1.4±0.5	1.0±0.2	**0.020**
LDL (mmol/L)	4.8±0.7 (n=9)	4.2±0.8	0.091
OxLDL (U/l)	56±18	51±12	0.475
LDL Vit E (µg/mg protein)	2.43±0.540	2.39±0.524	0.65
LDL particle size (nm)	0.24±0.02	0.24±0.03	0.387

Values are given as mean±standard deviation (±SD). Significance (p values) was calculated using a 2-tailed student t-test, and statistically significant differences are indicated by bold typeface.
* Chronic Kidney Disease

Table 2. List of lipid classes and sub-classes identified in LDL using dual polarity detection in a high resolution mass spectrometer by manual analyte identification using the Human Metabolome database.

Lipid Classes	Number of Mol. Ions Identified	Search Criteria	
		Formula	Adducts searched and ionization mode
Glycerolipids	**72**		
Triacylglycerols (TAG)	72	$C_nH_mNO_6$	$([M+NH_4]^+)$
Sterols and steroids	**14**		
Cholesterol (Chol)	1	C_nH_mO	$([M+H-H_2O]^+)$
Cholesterol sulphates (CS)	4	$C_nH_mO_4S$	$([M-H]^-)$
Cholesteryl esters (CE)	8	$C_nH_mNO_2$	$([M+NH_4]^+)$
Steroid conjugates	1	$C_nH_mO_z$	$([M+H]^+)/([M-H]^-)$
Fatty acids	**24**		
Free fatty acids (FA)	24	$C_nH_mO_2$	$([M-H]^-)$
Sphingolipids	**96**		
Sphingomyelins (SM)	41	$C_nH_mN_2O_6P$	$([MH]^+)$
Ceramides (Cer)	15	$C_nH_mNO_5$	$([M+HCOO]^-)$
Hexosyl-Ceramides (HexCer)	8	$C_nH_mNO_8$	$([M-H]^-)$
Lactosyl-Ceramides (LacCer)	5	$C_nH_mNO_{13}$	$([M-H]^-)$
Acidic Glycosphingolipids (Sulfatides, ST)	27	$C_nH_mNO_{11\text{-}13}S$	$([M-H]^-)$
Glycerophospholipids	**140**		
Phosphatidylinositols (PI)	15	$C_nH_mO_{13}P$	$([M-H]^-)$
Phosphatidylglycerols (PG)	6	$C_nH_mO_{10}P$	$([M-H]^-)$
Phosphatidylethanolamines (PE)	47		
Diacyl-PE	*15*	$C_nH_mNO_8P$	$([M-H]^-)$
Plasmenyl-PE (pPE)	*32*	$C_nH_mNO_7P$	$([M-H]^-)$
Lyso-phosphatidylethanolamines (lyso-PE)	5	$C_nH_mNO_7P$	$([M-H]^-)$
Phosphatidylcholines (PC)	63		
Diacyl-PC	*41*	$C_nH_mNO_8P$	$([MH]^+)$
Plasmenyl/plasmanyl-PC (pPC)	*22*	$C_nH_mNO_7P$	$([MH]^+)$
Lyso-phosphatidylcholines (lyso-PC)	4	$C_nH_mNO_7P$	$([MH]^+)$
Lipid-related compounds	**6**		
Prenols	1	C_nH_mOz	$([M+H]^+)/([M-H]^-)$
N-acyltaurines (NAT)	5	$C_nH_mNO_4S$	$([M+H]^+)/([M-H]^-)$
TOTAL	**352**		

Table 3. Summary of classification of plasma from CKD patients and controls using lipids profiles measured in either positive or negative ion modes, or the merged data set. Results for calibration (Cal) and cross-validation (CV) are shown.

Data set	Q^2*	Correct classification, %**		Sensitivity‡		Specificity‡‡	
		Cal	CV	Cal	CV	Cal	CV
Lipids pos.	0.83	100	94	1	0.93	1	0.96
Lipids neg.	0.81	100	96	1	0.96	1	0.96
Merged data	0.79	100	98	1	0.97	1	1

* $Q^2 = 1 - \frac{\sum_i (y_i - \widehat{y_i})^2}{\sum_i (y_i - \bar{y})^2}$

** Correct classification – percentage of cases assigned to correct classes
‡ Sensitivity = True Positives/(True Positives + False Negatives)
‡‡ Specificity = True Negative/(True Negatives + False Positives)

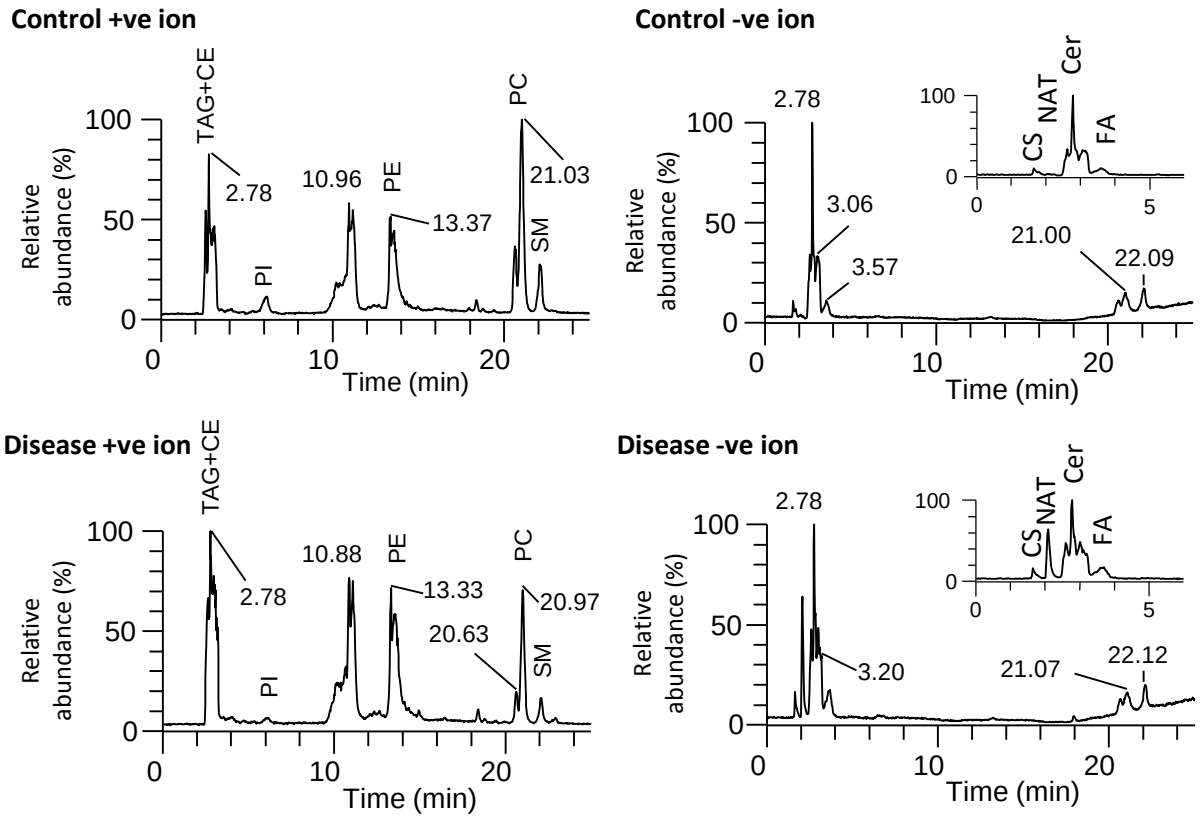

Figure 1. Typical normal-phase LC-MS chromatograms of normolipidemic LDL lipid extract (Control, top) and CKD patients (Disease, bottom) in positive (+ve, left) and negative (-ve, right) ion mode. Lipid extracts were prepared according to the Folch method and chromatograms were normalized to relative intensity (%). Labelled peaks are triacyglycerides and cholesteryl esters (TAG+CE), phosphatidylinositols (PI), phosphatidylethanolamines (PE), phosphatidylcholines (PC) and sphingomyelins (SM). The insets depict a zoomed region for the elution of cholesterol sulphate (CS), N-acyltaurines (NAT), ceramides (Cer) and fatty acids (FA) in negative ion mode.

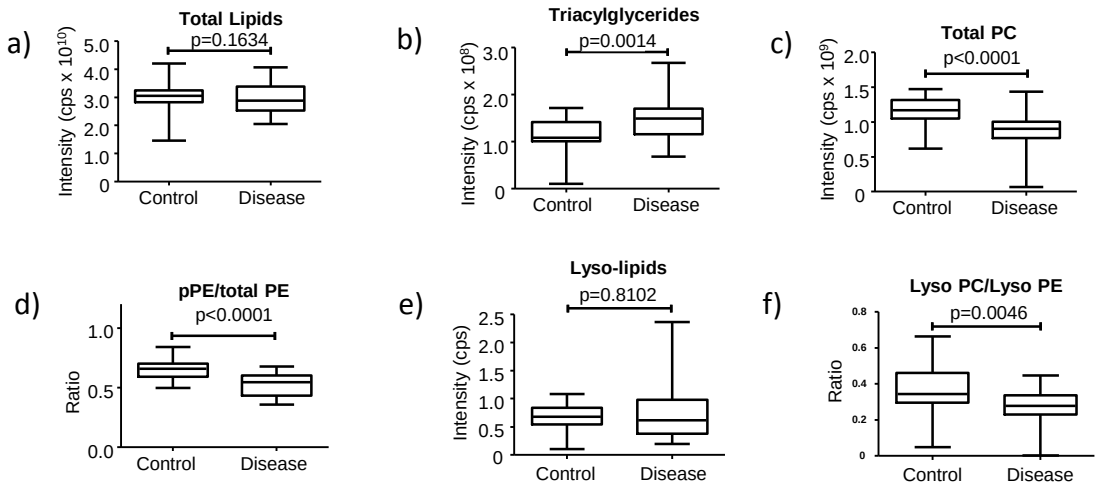

Figure 2. Box plots showing changes in major lipids in the disease group (n=10) against the age-matched control group (n=10). Samples were analysed in triplicate (n=3) and statistical analysis was carried out using the Mann-Whitney test to estimate the P values. Differences were considered statistically significant at $p<0.05$. Plots are a) total lipids detected; b) triacylglycerides; c) total phosphatidylcholine; d) ratio of plasmenyl ethanolamine to total phosphatidyl-ethanolamine; e) total lyso-phosphatidylcholine and lyso-phosphatidylethanolamine; f) ratio of lyso-phosphatidylcholine to lyso-phosphatidylethanolamine.

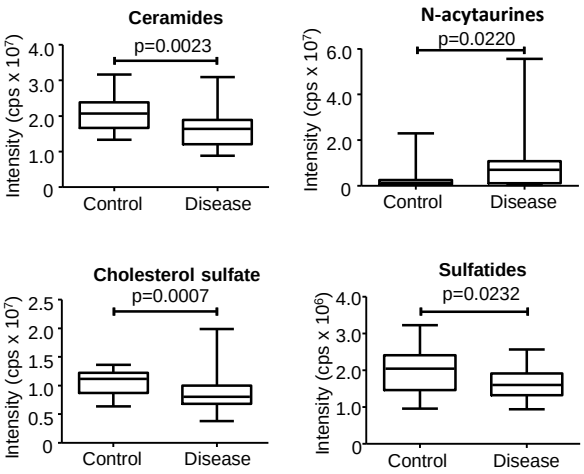

Figure 3. Box plots of minor lipids that showed significant change in CKD. Samples from the CKD group (n=10) and the age-matched control group (n=10) were analysed in triplicate and statistical analysis was carried out using the Mann-Whitney test to estimate the p values. Differences were considered statistically significant at $p<0.05$. The plots are a) ceramides; b) N-acyltaurines; c) cholesteryl sulphate; d) sulfatides.

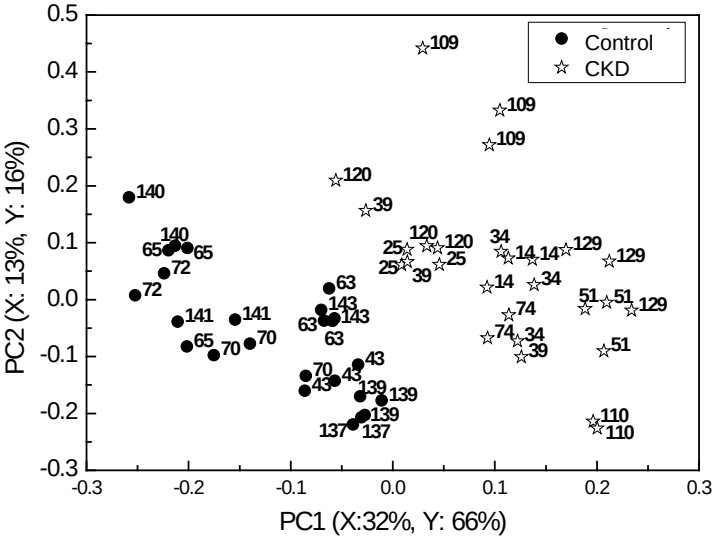

Figure 4. PLSDA scores plot for merged data (lipids detected in positive and negative ion mode). Numbers adjacent to the symbols are patient sample codes.

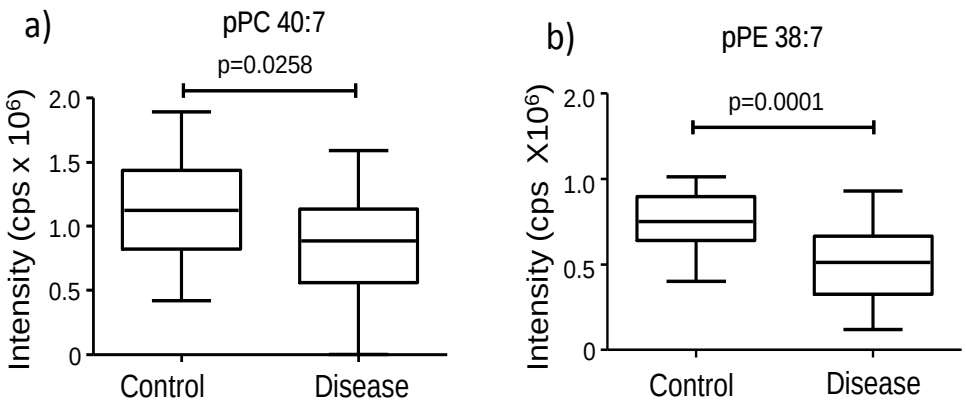

Figure 5. Boxplots of 2 individual lipid species that were altered in positive (PC) and negative ion mode (PE). Samples from the CKD group (n=10) and age-matched control group (n=10) were analysed in triplicate and statistical analysis was carried out using the Mann-Whitney test to estimate the p values. Differences were considered statistically significant at $p<0.05$. Plots are a) plasmenyl PC 40:7 and b) plasmenyl PE 38:7, where the numbers (C:n) correspond to the total number of carbon atoms: number of double bonds present in the acyl and alkyl chains (including the vinyl ether bond).

Supplemental Information

PLSDA Statistical analysis

PLSDA is one of the most commonly used classification methods for analysis of omics data, especially metabolomics. It is based on the Partial Least Square regression (PLS) approach and consists of using standard PLS algorithm with dummy dependent y variables containing class labels. As our data is a two-class case, control and disease, the values of the dependent variable were given as 1 for one class and -1 for the other class. PLSDA can be prone to overfit data, and so rigorous validation was undertaken. Optimization and validation of the PLSDA classification model and assessment of model quality were carried out using a cross validation and permutation test, using Q^2 as a measure of quality of the model. Cross-validation ensured that optimization and validation remained independent of each other. The statistical significance of the PLSDA classification model was assessed using a permutation test (1, 2). Permutation testing consists in changing randomly the order of the rows in the data set so the class labels are assigned randomly to the measurements. The classification model is then recalculated using this permuted data set. Permutation test considers the null hypothesis that a given classification model is not significant and describes noise. If null hypothesis is true, there should be no difference in the value of the quality-of-fit criteria between original data set and permuted one. After permuting the data and repeating calculations a sufficient number of times a null hypothesis (H0) distribution of the quality-of-fit criterion is obtained. For the results to be considered significant, the value of the quality-of-fit criterion for the original, non-permuted data set should be outside either the 95 or 99% confidence bounds of the H0 distribution of the values generated from the permuted data.

In the present study data were permuted 1000 times and Q^2 was used as quality-of-fit criterion for the permutation test. Q^2 is based on an evaluation of the error between the predicted and known variables, and was calculated using the following formula (38):

$$Q^2 = 1 - \frac{\sum_i (y_i - \hat{y}_i)^2}{\sum_i (y_i - \bar{y})^2},$$

where y_i is a value for the i^{th} sample, $\bar{y}_i$is a predicted value for the i^{th} sample and $\bar{y}$ is the mean y value.

Selection of the lipid species contributing to the discrimination between CKD patient and control groups was achieved using the Variable Importance in Projection (VIP) (36), which is effectively the weighted sum of the squares of the weight in the PLS analysis, and allows ranking of the variables according to their importance in the PLS model.VIP takes into account amount of the variance explained by the variable for each latent variables extracted and covariance between this variable and dependent variable y.

VIP of the j^{th} variable, VIP_j, for the model with K latent variables is calculated using the following equation:

$$VIP_j = \sqrt{\frac{p \sum_{k=1}^{K} (b_k^2 \mathbf{t_k}' \mathbf{t_k})(w_{jk})^2}{\sum_{k=1}^{K} (b_k^2 \mathbf{t_k}' \mathbf{t_k})}},$$

where p is a total number of variables in the model, $\mathbf{t_k}$ and b_k are scores and regression coefficient for the k^{th} latent variable, respectively, and w_{jk} is a weight for the j^{th} variable and k^{th} latent variable.

A VIP cut-off value of 0.85 was used for the merged set. The final classification model included 48 species detected in the positive mode and 55 in the negative mode.

PLSDA, permutation test and VIP algorithms were implemented in MATLAB, v. 7.12 (release 2011a).

1. Westerhuis, J. A., H. C. J. Hoefsloot, S. Smit, D. J. Vis, A. K. Smilde, E. J. J. van Velzen, J. P. M. van Duijnhoven, and F. A. van Dorsten. 2008. Assessment of PLSDA cross validation. *Metabolomics* **4**: 81-89.

2. Westerhuis, J. A., E. J. J. Velzen, H. C. J. Hoefsloot, and A. K. Smilde. 2008. Discriminant Q2 (DQ2) for improved discrimination in PLSDA models. *Metabolomics* **4**: 293-296.

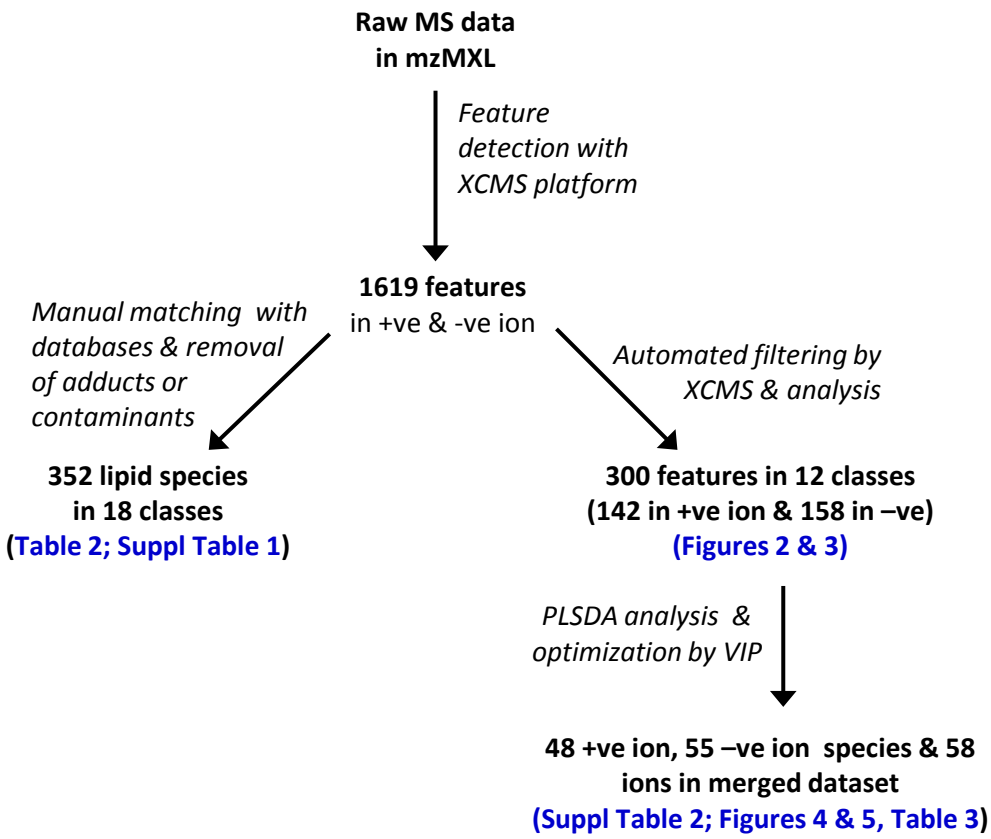

Supplemental Figure 1. Scheme showing the data processing approaches for MS data. The number of features identified in top-down LC-MS analysis of LDL from control and chronic kidney disease LDL, and the numbers of lipids identified at subsequent data processing stages, are given. The tables and figures in which these data sets are presented are indicated in blue.

Supplemental Table 1. List of ions observed in the averaged mass spectra (LC-MS) for each of the different lipid classes composing LDL population detected with polarity switching. The corresponding molecular formulae and proposed identifications of the lipid species are given, based on a mass error of <5 ppm between the experimental accurate mass and the calculated monoisotopic mass from the theoretical formula obtained using a home-built database and the Human Metabolome Project (HMDB). The *m/z* values used in this analysis were manual peak-top measurements, and may differ fractionally from the values quoted in Supplemental Table 2, which are mean *m/z* values from the automated extraction of features detected in at least 50% of data files, with error <2.5ppm and with 5s of retention time deviation. "d" indicates diacyl phospholipids and "p" indicates plasmanyl / plasmenyl phospholipids.

Lipid sub-classes	Molecular ions Analysed *m/z*	Molecular Formula	Tentative Lipid ID	Calculated Monoisotopic mass	Discrepancy (ppm)
Triacylglycerides (TAG)					
([M+NH$_4$]$^+$)	780.7076	$C_{48}H_{94}NO_6$	45:1	780.7081	0.7
	782.7230	$C_{48}H_{96}NO_6$	45:0	782.7238	1.0
	792.7075	$C_{49}H_{94}NO_6$	46:2	792.7081	0.8
	794.7230	$C_{49}H_{96}NO_6$	46:1	794.7238	1.0
	796.7396	$C_{49}H_{98}NO_6$	46:0	796.7394	0.2
	806.7241	$C_{50}H_{96}NO_6$	47:2	806.7238	0.4
	808.7386	$C_{50}H_{98}NO_6$	47:1	808.7394	1.0
	816.7079	$C_{51}H_{94}NO_6$	48:4	816.7081	0.3
	818.7234	$C_{51}H_{96}NO_6$	48:3	818.7238	0.4
	820.7382	$C_{51}H_{98}NO_6$	48:2	820.7394	1.5
	822.7543	$C_{51}H_{100}NO_6$	48:1	822.7551	0.9
	824.7708	$C_{51}H_{102}NO_6$	48:0	824.7707	0.1
	832.7392	$C_{52}H_{98}NO_6$	49:3	832.7394	0.3
	834.7538	$C_{52}H_{100}NO_6$	49:2	834.7551	1.5
	836.7705	$C_{52}H_{102}NO_6$	49:1	836.7707	0.3
	838.7861	$C_{52}H_{104}NO_6$	49:0	838.7864	0.3
	840.7083	$C_{53}H_{94}NO_6$	50:6	840.7081	0.2
	842.7238	$C_{53}H_{96}NO_6$	50:5	842.7238	0.0
	844.7392	$C_{53}H_{98}NO_6$	50:4	844.7394	0.3
	846.7545	$C_{53}H_{100}NO_6$	50:3	846.7551	0.7
	848.7696	$C_{53}H_{102}NO_6$	50:2	848.7707	1.3
	850.7863	$C_{53}H_{104}NO_6$	50:1	850.7864	0.1
	858.7540	$C_{54}H_{100}NO_6$	51:4	858.7551	1.2
	860.7701	$C_{54}H_{102}NO_6$	51:3	860.7707	0.7
	862.7848	$C_{54}H_{104}NO_6$	51:2	862.7864	1.8
	864.8020	$C_{54}H_{106}NO_6$	51:1	864.802	0.0
	866.7239	$C_{55}H_{96}NO_6$	52:7	866.7238	0.2
	868.7389	$C_{55}H_{98}NO_6$	52:6	868.7394	0.6
	870.7559	$C_{55}H_{100}NO_6$	52:5	870.7551	1.0
	872.7696	$C_{55}H_{102}NO_6$	52:4	872.7707	1.3
	874.7850	$C_{55}H_{104}NO_6$	52:3	874.7864	1.6
	876.7989	$C_{55}H_{106}NO_6$	52:2	876.802	3.6

	886.7846	$C_{56}H_{104}NO_6$	53:4	886.7864	2.0
	888.8011	$C_{56}H_{106}NO_6$	53:3	888.802	1.0
	890.7227	$C_{57}H_{96}NO_6$	54:9	890.7238	1.2
	890.8172	$C_{56}H_{108}NO_6$	53:2	890.8177	0.5
	892.7387	$C_{57}H_{98}NO_6$	54:8	892.7394	0.8
	894.7546	$C_{57}H_{100}NO_6$	54:7	894.7551	0.5
	896.7697	$C_{57}H_{102}NO_6$	54:6	896.7707	1.1
	898.7848	$C_{57}H_{104}NO_6$	54:5	898.7864	1.7
	900.8005	$C_{57}H_{106}NO_6$	54:4	900.802	1.7
	902.8173	$C_{57}H_{108}NO_6$	54:3	902.8177	0.4
	904.8325	$C_{57}H_{110}NO_6$	54:2	904.8333	0.9
	910.7844	$C_{58}H_{104}NO_6$	55:8	910.7864	2.2
	914.7239	$C_{59}H_{96}NO_6$	56:11	914.7238	0.1
	914.8156	$C_{58}H_{108}NO_6$	55:4	914.8177	2.3
	916.7394	$C_{59}H_{98}NO_6$	56:10	916.7394	0.0
	918.7544	$C_{59}H_{100}NO_6$	56:9	918.7551	0.7
	920.7700	$C_{59}H_{102}NO_6$	56:8	920.7707	0.8
	922.7848	$C_{59}H_{104}NO_6$	56:7	922.7864	1.7
	924.8010	$C_{59}H_{106}NO_6$	56:6	924.802	1.1
	926.8163	$C_{59}H_{108}NO_6$	56:5	926.8177	1.5
	928.8315	$C_{59}H_{110}NO_6$	56:4	928.8333	2.0
	930.8481	$C_{59}H_{112}NO_6$	56:3	930.849	0.9
	932.8620	$C_{59}H_{114}NO_6$	56:2	932.8646	2.8
	940.7394	$C_{61}H_{98}NO_6$	58:12	940.7394	0.0
	942.7545	$C_{61}H_{100}NO_6$	58:11	942.7551	0.6
	944.7698	$C_{61}H_{102}NO_6$	58:10	944.7707	1.0
	946.7851	$C_{61}H_{104}NO_6$	58:9	946.7864	1.3
	948.8004	$C_{61}H_{106}NO_6$	58:8	948.802	1.7
	950.8160	$C_{61}H_{108}NO_6$	58:7	950.8177	1.8
	952.8316	$C_{61}H_{110}NO_6$	58:6	952.8333	1.8
	954.8469	$C_{61}H_{112}NO_6$	58:5	954.849	2.2
	956.8622	$C_{61}H_{114}NO_6$	58:4	956.8646	2.5
	958.8788	$C_{61}H_{116}NO_6$	58:3	958.8803	1.5
	966.7548	$C_{63}H_{100}NO_6$	60:13	966.7551	0.3
	968.7703	$C_{63}H_{102}NO_6$	60:12	968.7707	0.4
	970.7851	$C_{63}H_{104}NO_6$	60:11	970.7864	1.3
	972.8011	$C_{63}H_{106}NO_6$	60:10	972.802	0.9
	990.7553	$C_{65}H_{100}NO_6$	62:15	990.7551	0.2
	992.7706	$C_{65}H_{102}NO_6$	62:14	992.7707	0.1
	994.7852	$C_{65}H_{104}NO_6$	62:13	994.7864	1.2
Cholesteryl Esters (CE)					
([M+NH$_4$]$^+$)	640.6039	$C_{43}H_{78}NO_2$	16:1	640.6033	1.0
	642.6180	$C_{43}H_{80}NO_2$	16:0	642.6189	1.4
	666.6179	$C_{45}H_{80}NO_2$	18:2	666.6189	1.5
	668.6346	$C_{45}H_{82}NO_2$	18:1	668.6346	0.1
	688.6022	$C_{47}H_{78}NO_2$	20:5	688.6033	1.5
	690.6181	$C_{47}H_{80}NO_2$	20:4	690.6189	1.2
	692.6376	$C_{47}H_{82}NO_2$	20:3	692.6346	4.4
	714.6182	$C_{49}H_{80}NO_2$	22:6	714.6189	1.0
Phosphatidylcholines (PC)*					
([MH]$^+$)	704.5239	$C_{38}H_{75}NO_8P$	*d*PC/30:1	704.5230	1.2
	706.5385	$C_{38}H_{77}NO_8P$	*d*PC/30:0	706.5387	0.3
	718.5751	$C_{40}H_{81}NO_7P$	*p*PC/32:1	718.5751	0.0
	720.5543	$C_{39}H_{79}NO_8P$	*d*PC/31:0	720.5543	0.0

	720.5909	$C_{40}H_{83}NO_7P$	*p*PC/32:0	720.5907	0.3
	730.5381	$C_{40}H_{77}NO_8P$	*d*PC/32:2	730.5387	0.8
	732.5532	$C_{40}H_{79}NO_8P$	*d*PC/32:1	732.5543	1.5
	734.5696	$C_{40}H_{81}NO_8P$	*d*PC/32:0	734.5700	0.5
	742.5743	$C_{42}H_{81}NO_7P$	*p*PC/34:3	742.5751	1.0
	744.5536	$C_{41}H_{79}NO_8P$	*d*PC/33:2	744.5543	1.0
	744.5910	$C_{42}H_{83}NO_7P$	*p*PC/34:2	744.5907	0.4
	746.5691	$C_{41}H_{81}NO_8P$	*d*PC/33:1	746.5700	1.2
	746.6065	$C_{42}H_{85}NO_7P$	*p*PC/34:1	746.6064	0.2
	748.5864	$C_{41}H_{83}NO_8P$	*d*PC/33:0	748.5856	1.0
	754.5381	$C_{42}H_{77}NO_8P$	*d*PC/34:4	754.5387	0.8
	756.5546	$C_{42}H_{79}NO_8P$	*d*PC/34:3	756.5543	0.4
	758.5685	$C_{42}H_{81}NO_8P$	*d*PC/34:2	758.57	2.0
	760.5851	$C_{42}H_{83}NO_8P$	*d*PC/34:1	760.5856	0.7
	762.6014	$C_{42}H_{85}NO_8P$	*d*PC/34:0	762.6013	0.2
	764.5617	$C_{44}H_{79}NO_7P$	*p*PC/36:6	764.5594	3.0
	766.5744	$C_{44}H_{81}NO_7P$	*p*PC/36:5	766.5751	0.9
	768.5904	$C_{44}H_{83}NO_7P$	*p*PC/36:4	768.5907	0.4
	770.6052	$C_{44}H_{85}NO_7P$	*p*PC/36:3	770.6064	1.5
	772.5842	$C_{43}H_{83}NO_8P$	*d*PC/35:2	772.5856	1.9
	772.6216	$C_{44}H_{87}NO_7P$	*p*PC/36:2	772.622	0.5
	774.5995	$C_{43}H_{85}NO_8P$	*d*PC/35:1	774.6013	2.3
	778.5364	$C_{44}H_{77}NO_8P$	*d*PC/36:6	778.5387	2.9
	780.5536	$C_{44}H_{79}NO_8P$	*d*PC/36:5	780.5543	0.9
	782.5693	$C_{44}H_{81}NO_8P$	*d*PC/36:4	782.57	0.9
	784.5844	$C_{44}H_{83}NO_8P$	*d*PC/36:3	784.5856	1.6
	786.5989	$C_{44}H_{85}NO_8P$	*d*PC/36:2	786.6013	3.0
	788.6154	$C_{44}H_{87}NO_8P$	*d*PC/36:1	788.6169	1.9
	790.5753	$C_{46}H_{81}NO_7P$	*p*PC/38:7	790.5751	0.3
	792.5547	$C_{45}H_{79}NO_8P$	*d*PC/37:6	792.5543	0.5
	792.5911	$C_{46}H_{83}NO_7P$	*p*PC/38:6	792.5907	0.5
	794.6056	$C_{46}H_{85}NO_7P$	*p*PC/38:5	794.6064	1.0
	796.5848	$C_{45}H_{83}NO_8P$	*d*PC/37:4	796.5856	1.0
	796.6214	$C_{46}H_{87}NO_7P$	*p*PC/38:4	796.622	0.8
	798.6375	$C_{46}H_{89}NO_7P$	*p*PC/38:3	798.6377	0.2
	800.6149	$C_{45}H_{87}NO_8P$	*d*PC/37:2	800.6169	2.5
	802.5383	$C_{46}H_{77}NO_8P$	*d*PC/38:8	802.5387	0.5
	804.5541	$C_{46}H_{79}NO_8P$	*d*PC/38:7	804.5543	0.3
	806.5696	$C_{46}H_{81}NO_8P$	*d*PC/38:6	806.57	0.5
	808.5849	$C_{46}H_{83}NO_8P$	*d*PC/38:5	808.5856	0.9
	810.5994	$C_{46}H_{85}NO_8P$	*d*PC/38:4	810.6013	2.3
	812.6160	$C_{46}H_{87}NO_8P$	*d*PC/38:3	812.6169	1.1
	814.6310	$C_{46}H_{89}NO_8P$	*d*PC/38:2	814.6326	1.9
	816.5912	$C_{48}H_{83}NO_7P$	*p*PC/40:8	816.5907	0.6
	818.6069	$C_{48}H_{85}NO_7P$	*p*PC/40:7	818.6064	0.7
	820.5853	$C_{47}H_{83}NO_8P$	*d*PC/39:6	820.5856	0.4
	820.6214	$C_{48}H_{87}NO_7P$	*p*PC/40:6	820.6220	0.8
	822.5656	$C_{46}H_{81}NO_9P$	*d*PC/38:6-OH	822.5649	0.9
	822.6372	$C_{48}H_{89}NO_7P$	*p*PC/40:5	822.6377	0.6
	828.5520	$C_{48}H_{79}NO_8P$	*d*PC/40:9	828.5543	2.8
	830.5707	$C_{48}H_{81}NO_8P$	*d*PC/40:8	830.5700	0.9
	832.5858	$C_{48}H_{83}NO_8P$	*d*PC/40:7	832.5856	0.2
	834.6025	$C_{48}H_{85}NO_8P$	*d*PC/40:6	834.6013	1.5
	836.6159	$C_{48}H_{87}NO_8P$	*d*PC/40:5	836.6169	1.2
	838.6317	$C_{48}H_{89}NO_8P$	*d*PC/40:4	838.6326	1.0

	846.6376	$C_{50}H_{89}NO_7P$	*p*PC/42:6	846.6377	0.1
	848.6529	$C_{50}H_{91}NO_7P$	*p*PC/42:5	848.6533	0.5
	850.6684	$C_{50}H_{93}NO_7P$	*p*PC/42:4	850.6690	0.7
	856.5851	$C_{50}H_{83}NO_8P$	*d*PC/42:9	856.5856	0.6
Lyso-phosphatidylcholines (Lyso-PC)					
([MH]$^+$)	496.3403	$C_{24}H_{51}NO_7P$	16:0	496.3403	0.0
	520.3408	$C_{26}H_{51}NO_7P$	18:2	520.3403	0.9
	522.3561	$C_{26}H_{53}NO_7P$	18:1	522.3560	0.3
	524.3718	$C_{26}H_{55}NO_7P$	18:0	524.3716	0.4
Sphingomyelins (SM)**					
([MH]$^+$)	647.5128	$C_{35}H_{72}N_2O_6P$	30:1	647.5128	0.0
	661.5283	$C_{36}H_{74}N_2O_6P$	31:1	661.5284	0.2
	673.5287	$C_{37}H_{74}N_2O_6P$	32:2	673.5284	0.4
	675.5431	$C_{37}H_{76}N_2O_6P$	32:1	675.5441	1.5
	689.5598	$C_{38}H_{78}N_2O_6P$	33:2	689.5597	0.1
	691.5758	$C_{38}H_{80}N_2O_6P$	33:1	691.5754	0.6
	701.5598	$C_{39}H_{78}N_2O_6P$	34:2	701.5597	0.1
	703.5738	$C_{39}H_{80}N_2O_6P$	34:1	703.5754	2.3
	705.5909	$C_{39}H_{82}N_2O_6P$	34:1	705.5910	0.2
	715.5750	$C_{40}H_{80}N_2O_6P$	35:2	715.5754	0.6
	717.5905	$C_{40}H_{82}N_2O_6P$	35:1	717.5910	0.8
	719.5707	$C_{39}H_{80}N_2O_7P$	34:1-OH	719.5703	0.5
	725.5570	$C_{41}H_{78}N_2O_6P$	36:4	725.5597	3.8
	727.5742	$C_{41}H_{80}N_2O_6P$	36:3	727.5754	1.6
	729.5911	$C_{41}H_{82}N_2O_6P$	36:2	729.5910	0.1
	731.6053	$C_{41}H_{84}N_2O_6P$	36:1	731.6067	1.9
	733.6220	$C_{41}H_{86}N_2O_6P$	36:0	733.6224	0.5
	743.6063	$C_{42}H_{84}N_2O_6P$	37:0	743.6067	0.5
	745.6219	$C_{42}H_{86}N_2O_6P$	37:1	745.6224	0.6
	753.5886	$C_{43}H_{82}N_2O_6P$	38:4	753.5910	3.3
	755.6064	$C_{43}H_{84}N_2O_6P$	38:3	755.6067	0.4
	757.6223	$C_{43}H_{86}N_2O_6P$	38:2	757.6224	0.1
	759.6383	$C_{43}H_{88}N_2O_6P$	38:1	759.6380	0.4
	771.6379	$C_{44}H_{88}N_2O_6P$	39:2	771.6380	0.1
	773.6538	$C_{44}H_{90}N_2O_6P$	39:1	773.6537	0.2
	779.6037	$C_{45}H_{84}N_2O_6P$	40:5	779.6067	3.8
	781.6202	$C_{45}H_{86}N_2O_6P$	40:4	781.6224	2.8
	783.6381	$C_{45}H_{88}N_2O_6P$	40:3	783.6380	0.1
	785.6539	$C_{45}H_{90}N_2O_6P$	40:2	785.6537	0.3
	787.6678	$C_{45}H_{92}N_2O_6P$	40:1	787.6693	1.9
	797.6537	$C_{46}H_{90}N_2O_6P$	41:3	797.6537	0.1
	799.6690	$C_{46}H_{92}N_2O_6P$	41:2	799.6693	0.4
	801.6846	$C_{46}H_{94}N_2O_6P$	41:1	801.6850	0.4
	811.6691	$C_{47}H_{92}N_2O_6P$	42:3	811.6693	0.2
	813.6832	$C_{47}H_{94}N_2O_6P$	42:2	813.6850	2.2
	815.7000	$C_{47}H_{96}N_2O_6P$	42:1	815.7006	0.7
	825.6850	$C_{48}H_{94}N_2O_6P$	43:3	825.6850	0.1
	827.6995	$C_{48}H_{96}N_2O_6P$	43:2	827.7006	1.3
	833.6512	$C_{49}H_{90}N_2O_6P$	44:5	833.6537	2.9
	835.6658	$C_{49}H_{92}N_2O_6P$	44:4	835.6693	4.2
	839.7008	$C_{49}H_{96}N_2O_6P$	44:3	839.7006	0.2
Ceramides (Cer)**					

([M+HCOO$^-$])	582.5100	$C_{35}H_{68}NO_5$	34:1	582.5097	0.4
	610.5413	$C_{37}H_{72}NO_5$	36:1	610.5410	0.4
	638.5725	$C_{39}H_{76}NO_5$	38:1	638.5723	0.2
	652.5893	$C_{40}H_{78}NO_5$	39:1	652.5880	2.0
	664.5880	$C_{41}H_{78}NO_5$	40:2	664.5880	0.0
	666.6037	$C_{41}H_{80}NO_5$	40:1	666.6036	0.1
	678.6034	$C_{42}H_{80}NO_5$	41:2	678.6036	0.4
	680.6190	$C_{42}H_{82}NO_5$	41:1	680.6193	0.4
	692.6190	$C_{43}H_{82}NO_5$	42:2	692.6193	0.4
	694.6345	$C_{43}H_{84}NO_5$	42:1	694.6349	0.6
	706.6346	$C_{44}H_{84}NO_5$	43:1	706.6349	0.5
	708.6506	$C_{44}H_{86}NO_5$	43:1	708.6506	0.0
	710.6311	$C_{43}H_{84}NO_6$	42:1-OH	710.6299	1.7
	720.6504	$C_{45}H_{86}NO_5$	44:2	720.6506	0.3
	722.6651	$C_{45}H_{88}NO_5$	44:1	722.6662	1.6
HexosylCeramide**					
([M+HCOO$^-$])	744.5623	$C_{41}H_{78}NO_{10}$	34:1	744.5626	0.4
	826.6404	$C_{47}H_{88}NO_{10}$	40:2	826.6408	0.5
	828.6559	$C_{47}H_{90}NO_{10}$	40:1	828.6565	0.7
	840.6564	$C_{48}H_{90}NO_{10}$	41:2	840.6565	0.1
	842.6718	$C_{48}H_{92}NO_{10}$	41:1	842.6721	0.4
	854.6719	$C_{49}H_{92}NO_{10}$	42:2	854.6721	0.3
	856.6874	$C_{49}H_{94}NO_{10}$	42:1	856.6878	0.4
	868.6874	$C_{50}H_{94}NO_{10}$	43:2	868.6878	0.4
LactosylCeramides**					
([M-H$^-$])	832.5779	$C_{44}H_{82}NO_{13}$	32:1	832.5786	0.9
	858.5935	$C_{46}H_{84}NO_{13}$	34:2	858.5943	0.9
	860.6090	$C_{46}H_{86}NO_{13}$	34:1	860.6099	1.1
	886.6249	$C_{48}H_{88}NO_{13}$	36:2	886.6256	0.8
	970.7190	$C_{54}H_{100}NO_{13}$	42:2	970.7195	0.5
Sulfatides (ST)**					
([M-H$^-$])	750.4828	$C_{38}H_{72}NO_{11}S$	32:1	750.4826	0.3
	764.4977	$C_{39}H_{74}NO_{11}S$	33:1	764.4983	0.7
	766.4771	$C_{38}H_{72}NO_{12}S$	32:1-OH	766.4775	0.6
	776.4979	$C_{40}H_{74}NO_{11}S$	34:1	776.4983	0.5
	778.5134	$C_{40}H_{76}NO_{11}S$	34:0	778.5139	0.7
	792.4926	$C_{40}H_{74}NO_{12}S$	34:1-OH	792.4932	0.7
	794.5084	$C_{40}H_{76}NO_{12}S$	34:0-OH	794.5088	0.5
	812.5189	$C_{40}H_{78}NO_{13}S$	-	812.5194	0.6
	832.5598	$C_{44}H_{82}NO_{11}S$	38:2	832.5609	1.3
	834.5763	$C_{44}H_{84}NO_{11}S$	38:1	834.5765	0.2
	850.5721	$C_{44}H_{84}NO_{12}S$	38:1-OH	850.5714	0.8
	860.5922	$C_{46}H_{86}NO_{11}S$	40:2	860.5922	0.0
	862.6085	$C_{46}H_{88}NO_{11}S$	40:1	862.6078	0.8
	874.6069	$C_{47}H_{88}NO_{11}S$	41:1	874.6078	1.0
	876.5873	$C_{46}H_{86}NO_{12}S$	40:2-OH	876.5871	0.3
	878.6031	$C_{46}H_{88}NO_{12}S$	40:1-OH	878.6027	0.4
	886.6074	$C_{48}H_{88}NO_{11}S$	42:3	886.6078	0.5
	888.6233	$C_{48}H_{90}NO_{11}S$	42:2	888.6235	0.2
	892.6179	$C_{47}H_{90}NO_{12}S$	41:0-OH	892.6184	0.5
	896.6132	$C_{46}H_{90}NO_{13}S$	40:0-$(OH)_2$	896.6133	0.1
	902.6030	$C_{48}H_{88}NO_{12}S$	42:3-OH	902.6027	0.3
	904.6180	$C_{48}H_{90}NO_{12}S$	42:2-OH	904.6184	0.4
	906.6342	$C_{48}H_{92}NO_{12}S$	42:1-OH	906.6340	0.2
	920.6136	$C_{48}H_{90}NO_{13}S$	42:2-$(OH)_2$	920.6133	0.3

	922.6289	$C_{48}H_{92}NO_{13}S$	42:1-$(OH)_2$	922.6289	0.0
	932.6473	$C_{50}H_{94}NO_{12}S$	44:2-OH	932.6497	2.5
	1010.5651	$C_{56}H_{84}NO_{13}S$	-	1010.5663	1.2
Free Fatty Acids (FA) and conjugates					
([M-H]$^-$)	227.2017	$C_{14}H_{27}O_2$	14:0	227.2011	2.6
	241.2174	$C_{15}H_{29}O_2$	15:0	241.2168	2.7
	253.2173	$C_{16}H_{29}O_2$	16:1	253.2168	2.2
	255.2328	$C_{16}H_{31}O_2$	16:0	255.2324	1.5
	267.2329	$C_{17}H_{31}O_2$	17:1	267.2324	1.9
	269.2486	$C_{17}H_{33}O_2$	17:0	269.2481	2.0
	277.2173	$C_{18}H_{29}O_2$	18:3	277.2168	2.0
	279.2330	$C_{18}H_{31}O_2$	18:2	279.2324	2.1
	281.2486	$C_{18}H_{33}O_2$	18:1	281.2481	1.9
	283.2640	$C_{18}H_{35}O_2$	18:0	283.2637	1.0
	297.2434	$C_{18}H_{33}O_3$	18:1-OH	297.2430	1.4
	303.2329	$C_{20}H_{31}O_2$	20:4	303.2324	1.6
	305.2489	$C_{20}H_{33}O_2$	20:3	305.2481	2.8
	307.2646	$C_{20}H_{35}O_2$	20:2	307.2637	2.9
	319.2278	$C_{20}H_{31}O_3$	20:4-OH	319.2273	1.5
	327.2330	$C_{22}H_{31}O_2$	22:6	327.2324	1.8
	331.2643	$C_{22}H_{35}O_2$	22:4	331.2637	1.8
	367.3581	$C_{24}H_{47}O_2$	24:0	367.3576	1.3
	369.3010	$C_{22}H_{41}O_4$	22:1-OH	369.3005	1.4
	381.3739	$C_{25}H_{49}O_2$	25:0	381.3733	1.7
	395.3893	$C_{26}H_{51}O_2$	26:0	395.3889	1.0
	409.4051	$C_{27}H_{53}O_2$	27:0	409.4046	1.3
	423.4208	$C_{28}H_{55}O_2$	28:0	423.4202	1.4
	449.3630	$C_{28}H_{49}O_4$	28:3-OH	449.3631	0.2
Phosphatidylinositols (PI)					
([M-H]$^-$)	807.5018	$C_{41}H_{76}O_{13}P$	32:1	807.5024	0.7
	809.5166	$C_{41}H_7O_{13}P$	32:0	809.5180	1.7
	833.5175	$C_{43}H_{78}O_{13}P$	34:2	833.5180	0.6
	835.5333	$C_{43}H_{80}O_{13}P$	34:1	835.5337	0.4
	847.5692	$C_{45}H_{84}O_{12}P$	35:2	847.5700	1.0
	857.5180	$C_{45}H_{78}O_{13}P$	36:4	857.5180	0.0
	859.5334	$C_{45}H_{80}O_{13}P$	36:3	859.5337	0.3
	861.5490	$C_{45}H_{82}O_{13}P$	36:2	861.5493	0.4
	863.5644	$C_{45}H_{84}O_{13}P$	36:1	863.5650	0.6
	871.5320	$C_{46}H_{80}O_{13}P$	37:4	871.5337	1.9
	881.5187	$C_{47}H_{78}O_{13}P$	38:6	881.5180	0.8
	883.5332	$C_{47}H_{80}O_{13}P$	38:5	883.5337	0.5
	885.5489	$C_{47}H_{82}O_{13}P$	38:4	885.5493	0.5
	909.5486	$C_{49}H_{82}O_{13}P$	40:6	909.5493	0.8
	911.5642	$C_{49}H_{84}O_{13}P$	40:5	911.5650	0.8
Phosphatidyl-ethanolamines (PE)*					
([M-H]$^-$)	698.5125	$C_{39}H_{73}NO_7P$	*p*PE/34:3	698.5125	0.0
	700.5282	$C_{39}H_{75}NO_7P$	*p*PE/34:2	700.5281	0.1
	702.5436	$C_{39}H_{77}NO_7P$	*p*PE/34:1	702.5438	0.2
	712.5284	$C_{40}H_{75}NO_7P$	*p*PE/35:3	712.5281	0.4
	714.5074	$C_{39}H_{73}NO_8P$	*d*PE/34:2	714.5074	0.0
	716.5237	$C_{39}H_{75}NO_8P$	*d*PE/34:1	716.5230	0.9
	720.4967	$C_{41}H_{71}NO_7P$	*p*PE/36:6	720.4968	0.2

	722.5121	$C_{41}H_{73}NO_7P$	*p*PE/36:5	722.5125	0.5
	724.5280	$C_{41}H_{75}NO_7P$	*p*PE/36:4	724.5281	0.2
	726.5440	$C_{41}H_{77}NO_7P$	*p*PE/36:3	726.5438	0.3
	728.5593	$C_{41}H_{79}NO_7P$	*p*PE/36:2	728.5594	0.2
	730.5753	$C_{41}H_{81}NO_7P$	*p*PE/36:1	730.5751	0.3
	732.4960	$C_{42}H_{71}NO_7P$	*p*PE/37:7	732.4968	1.1
	734.5123	$C_{42}H_{73}NO_7P$	*p*PE/37:6	734.5125	0.2
	736.4918	$C_{41}H_{71}NO_8P$	*d*PE/36:5	736.4917	0.1
	736.5280	$C_{42}H_{75}NO_7P$	*p*PE/37:5	736.5281	0.2
	738.5072	$C_{41}H_{73}NO_8P$	*d*PE/36:4	738.5074	0.2
	740.5230	$C_{41}H_{75}NO_8P$	*d*PE/36:3	740.5230	0.0
	742.5385	$C_{41}H_{77}NO_8P$	*d*PE/36:2	742.5387	0.2
	744.4969	$C_{43}H_{71}NO_7P$	*p*PE/38:8	744.4968	0.1
	744.5547	$C_{41}H_{79}NO_8P$	*d*PE/36:1	744.5543	0.5
	746.5121	$C_{43}H_{73}NO_7P$	*p*PE/38:7	746.5125	0.5
	748.5271	$C_{43}H_{75}NO_7P$	*p*PE/38:6	748.5281	1.4
	750.5421	$C_{43}H_{77}NO_7P$	*p*PE/38:5	750.5438	2.2
	752.5592	$C_{43}H_{79}NO_7P$	*p*PE/38:4	752.5594	0.3
	756.5908	$C_{43}H_{83}NO_7P$	*p*PE/38:3	756.5907	0.1
	760.5270	$C_{44}H_{75}NO_7P$	*p*PE/39:6	760.5281	1.5
	762.5066	$C_{43}H_{73}NO_8P$	*d*PE/38:6	762.5074	1.0
	764.5225	$C_{43}H_{75}NO_8P$	*d*PE/38:5	764.5230	0.7
	766.5383	$C_{43}H_{77}NO_8P$	*d*PE/38:4	766.5387	0.5
	768.5543	$C_{43}H_{79}NO_8P$	*d*PE/38:3	768.5543	0.0
	772.5269	$C_{45}H_{75}NO_7P$	*p*PE/40:8	772.5281	1.6
	774.5424	$C_{45}H_{77}NO_7P$	*p*PE/40:7	774.5438	1.8
	776.5590	$C_{45}H_{79}NO_7P$	*p*PE/40:6	776.5594	0.5
	778.5746	$C_{45}H_{81}NO_7P$	*p*PE/40:5	778.5751	0.6
	780.5908	$C_{45}H_{83}NO_7P$	*p*PE/40:4	780.5907	0.1
	782.6067	$C_{45}H_{85}NO_7P$	*p*PE/40:3	782.6064	0.4
	788.5220	$C_{45}H_{75}NO_8P$	*d*PE/40:7	788.5230	1.3
	790.5377	$C_{45}H_{77}NO_8P$	*d*PE/40:6	790.5387	1.2
	792.5537	$C_{45}H_{79}NO_8P$	*d*PE/40:5	792.5543	0.8
	800.5583	$C_{47}H_{79}NO_7P$	*p*PE/42:8	800.5594	1.4
	802.5741	$C_{47}H_{81}NO_7P$	*p*PE/42:7	802.5751	1.2
	808.6212	$C_{47}H_{87}NO_7P$	*p*PE/42:4	808.6220	1.0
	826.5744	$C_{49}H_{81}NO_7P$	*p*PE/44:8	826.5751	0.8
	828.5902	$C_{49}H_{83}NO_7P$	*p*PE/44:7	828.5907	0.6
	830.6055	$C_{49}H_{85}NO_7P$	*p*PE/44:6	830.6064	1.0
	832.6214	$C_{49}H_{87}NO_7P$	*p*PE/44:5	832.6220	0.7
Lyso-phosphatidylethanolamines (lyso-PE)					
([M-H]⁻)	452.2792	$C_{21}H_{43}NO_7P$	16:0	452.2777	3.3
	464.3144	$C_{23}H_{47}NO_6P$	p18:0	464.3141	0.6
	476.2783	$C_{23}H_{43}NO_7P$	18:2	476.2777	1.2
	478.2935	$C_{23}H_{45}NO_7P$	18:1	478.2934	0.3
	480.3094	$C_{23}H_{47}NO_7P$	18:0	480.3090	0.8
Phosphatidylglycerol (PG)					
([M-H]⁻)	743.4851	$C_{40}H_{72}O_{10}P$	34:3	743.4863	1.6
	745.5018	$C_{40}H_{74}O_{10}P$	34:2	745.5020	0.2
	747.5179	$C_{40}H_{76}O_{10}P$	34:1	747.5176	0.4
	771.5167	$C_{42}H_{76}O_{10}P$	36:3	771.5176	1.2
	773.5325	$C_{42}H_{78}O_{10}P$	36:2	773.5333	1.0

	775.5483	$C_{42}H_{80}O_{10}P$	36:1	775.5489	0.8
Sterols and Steroid derivatives					
([M-H$_2$O+H]$^+$)	369.3516	$C_{27}H_{45}$	n/a	369.3521	1.4
([M-H]$^-$)	409.3106	$C_{28}H_{41}O_2$		409.3107	0.1
Cholesterol sulphates ([M-H]$^-$)	465.3041	$C_{27}H_{45}O_4S$		465.3039	0.5
	479.3199	$C_{28}H_{47}O_4S$		479.3195	0.8
	493.3357	$C_{29}H_{49}O_4S$		493.3352	1.1
	507.3515	$C_{30}H_{51}O_4S$		507.3508	1.4
Other lipid-like compounds					
([M+HCOO]$^-$)	395.2437	$C_{22}H_{35}O_6$		395.2434	0.9
Lipoamino acids (N-acyltaurines)					
([M-H]$^-$)	376.2528	$C_{19}H_{38}NO_4S$	16:0	376.2522	1.7
	390.2682	$C_{20}H_{40}NO_4S$	18:0	390.2678	1.0
	400.2526	$C_{21}H_{38}NO_4S$	18:2	400.2522	1.1
	402.2679	$C_{21}H_{40}NO_4S$	18:1	402.2678	0.2
	430.2995	$C_{23}H_{44}NO_4S$	20:0	430.2991	0.9

[a] The structures (C:n) are proposed based on the total number of carbons that compose the fatty acyl chains and the total number of double bonds that may be considered for the m/z value observed.

* Plasmalogen phospholipid species may contain the contribution of alkyl- or alkenyl-acyl.

** Compounds may contain the contribution of sphin-4-enine or sphinganine structure.

Supplemental Table 2. Identification of lipid species that were found to be discriminating for CKD using PLSDA. A final cut-off of 0.85 for the significance factor was used. Rt med and *m/z* med correspond to the averaged retention time and mass-to-charge ratio of an identified feature from all chromatographic runs in which the feature was identified. The lipid species were identified by matching the experimental m/z to the calculated monoisotopic mass to within 5 ppm mass accuracy. The *m/z* values quoted in this table are mean *m/z* values from the automated extraction of features, and hence may differ fractionally from the manual peak-top m/z values quoted in Supplemental Table 1. "d" indicates diacyl phospholipids and "p" indicates plasmanyl / plasmenyl phospholipids.

Lipids in Positive Ion Mode				
Lipid Class	**Chain length: double bonds**	***m/z* med**	**Rt med**	**Significance parameter**
pPC	**36:6**	764.5601	19.539	1.47
dPC	**36:5**	780.5551	19.579	1.45
dPC	**37:4**	796.5862	19.589	1.38
dPC	**32:1**	732.5549	20.083	1.36
TAG	**52:4**	872.7706	2.532	1.32
SM	**36:1**	731.6062	21.065	1.27
TAG	**52:3**	874.7861	2.579	1.25
SM	**39:1**	773.6537	21.059	1.23
dPC	**38:6**	806.5703	19.507	1.22
TAG	**54:4**	900.8015	2.564	1.19
dPC	**39:6**	820.5851	19.492	1.18
dPC	**40:6**	834.6006	19.488	1.14
TAG	**54:3**	902.8172	2.626	1.13
pPC	**38:7**	790.5761	19.472	1.11
dPC	**38:4**	810.6004	19.577	1.11
dPC	**34:3**	756.5552	19.901	1.11
pPC	**40:7**	818.6061	19.554	1.09
dPC	**36:6**	778.5388	19.573	1.05
dPC	**36:5**	780.5518	19.975	1.05
TAG	**54:5**	898.7860	2.532	1.05
TAG	**58:8**	948.8015	2.510	1.05
SM	**42:3**	811.6693	20.885	1.03
pPC	**42:5**	848.6522	19.782	1.03
TAG	**56:7**	922.7866	2.978	1.02
dPC	**38:8**	802.5370	19.578	1.02
dPC	**36:0**	790.6231	20.081	1.00
dPC	**40:0**	828.5513	19.506	1.00
TAG	**55:4**	914.7815	2.509	0.99
dPC	**38:5**	808.5836	19.536	0.97
SM	**35:1**	717.5906	21.085	0.97
TAG	**58:9**	846.7552	2.535	0.97
dPC	**32:2**	730.5393	20.038	0.95
dPC	**33:1**	746.5715	20.063	0.94
dPC	**36:1**	788.6115	20.039	0.92

dPC	**38:3**	812.6077	19.576	0.92
SM	**36:3**	727.5631	21.123	0.91
dPC	**30:1**	704.5242	20.127	0.91
SM	**38:2**	757.6225	20.938	0.91
SM	**38:1**	759.6377	21.050	0.90
SM	**38:0**	761.6439	21.047	0.90
TAG	**52:6**	870.7554	2.510	0.89
TAG	**55:3**	916.7966	2.509	0.88
TAG	**58:7**	950.8161	2.529	0.88
PC	**/**	708.5452	20.255	0.87
SM	**36:0**	733.6126	21.055	0.87
TAG	**52:1**	878.8094	2.642	0.87
SM	**36:2**	729.5910	20.984	0.87
dPC	**40:8**	830.5681	19.507	0.86

Lipids in Negative Ion Mode

Lipid Class	Chain length: double bonds	m/z med	Rt med	Significance parameter
dPC	**32:1**	776.5450	21.178	1.78
Cer	**/**	698.6227	2.821	1.51
pPE	**36:6**	720.4984	13.133	1.50
dPC	**36:5**	824.5448	20.684	1.48
dPC	**36:6**	822.5294	20.643	1.45
dPE	**34:2**	714.5093	13.647	1.28
dPC	**34:4**	798.5285	20.775	1.24
pPE	**38:7**	746.5137	13.032	1.23
dPE	**36:3**	740.5247	13.512	1.16
dPE	**34:1**	716.5259	13.687	1.15
SM	**36:2**	773.5816	22.011	1.14
dPE	**38:4**	752.5509	13.086	1.13
dPC	**34:0**	806.5823	21.158	1.13
dPC	**34:1**	804.5748	21.145	1.12
dPE	**36:4**	738.5090	13.275	1.12
SM	**42:3**	855.6594	21.880	1.11
SM	**41:3**	841.6440	21.866	1.11
dPC	**38:5**	852.5750	20.720	1.10
PC	**40:6**	878.5913	20.545	1.09
PC	**38:7**	848.5447	20.538	1.09
pPE	**40:7**	774.5451	12.965	1.08
SM	**36:1**	775.5968	22.085	1.07
SM	**34:1**	749.5820	21.968	1.07
dPC	**38:6**	850.5600	20.583	1.05
HexCer	**43:0**	872.6835	3.011	1.04
pPC	**36:3**	814.5966	21.210	1.04
Cer	**41:2**	678.6050	2.831	1.04

pPE	**38:5**	750.5450	13.090	1.03
dPC	**36:4**	826.5600	20.717	1.02
Cer	**44:1**	722.6675	2.817	1.01
dPE	**36:2**	742.5404	13.576	1.00
dPC	**38:6**	750.5295	21.341	1.00
dPC	**40:5**	790.5971	21.508	1.00
dPC	**32:2**	774.5295	21.109	1.00
HexCer	**41:1**	842.6727	3.041	1.00
dPE	**38:5**	764.5246	13.146	0.97
dPC	**30:3**	744.5555	21.133	0.97
SM	**30:2**	689.5519	22.129	0.97
dPE	**38:3**	768.5461	13.193	0.97
dPC	**34:3**	800.5448	20.985	0.97
Cer	**40:2**	664.5893	2.833	0.94
Cer	**34:1**	582.5108	2.874	0.92
HexCer	**42:2**	854.6725	3.029	0.92
Cer	**42:1**	694.6359	2.822	0.92
dPE	**38:6**	762.5085	13.157	0.91
SM	**30:1**	691.5037	22.254	0.90
dPE	**38:4**	766.5399	13.203	0.89
pPE	**40:8**	772.5293	12.917	0.89
pPE	**36:5**	722.5139	13.146	0.88
dPC	**38:3**	856.5981	20.665	0.87
Cer	**41:1**	680.6205	2.825	0.87
SM	**37:1**	789.6124	22.086	0.87
SM	**38:1**	803.6284	22.067	0.86
dPC	**28:0**	722.4984	21.359	0.85
SM	**34:1**	749.5720	22.139	0.84

Merged data set - Positive and Negative Ion Modes				
Lipid Class	**Chain length: double bonds**	**m/z med**	**Rt med**	**Significance parameter**
dPC	**32:1**	776.5450	21.178	1.38
pPC	**36:6**	764.5601	19.539	1.33
dPC	**36:5**	780.5551	19.579	1.31
TAG	**52:4**	872.7706	2.532	1.29
pPE	**36:6**	720.4984	13.133	1.24
PC	**32:1**	732.5549	20.083	1.22
TAG	**52:3**	874.7861	2.579	1.21
Cer	**/**	698.6227	2.821	1.20
TAG	**54:4**	900.8015	2.564	1.18
dPC	**36:6**	822.5294	20.643	1.13
dPC	**37:4**	796.5862	19.589	1.13
SM	**36:1**	731.6062	21.065	1.10
dPC	**36:5**	824.5448	20.684	1.10

dPE	**38:4**	752.5509	13.086	1.08
pPE	**38:7**	746.5137	13.032	1.07
TAG	**54:5**	898.7860	2.532	1.07
dPC	**38:6**	806.5703	19.507	1.07
dPC	**39:6**	820.5851	19.492	1.07
dPC	**40:6**	834.6006	19.488	1.05
TAG	**54:3**	902.8172	2.626	1.05
dPC	**36:0**	790.5761	19.472	1.03
PC	**40:6**	878.5913	20.545	1.02
dPC	**34:4**	798.5285	20.775	1.01
dPC	**38:8**	802.5370	19.578	1.01
dPC	**38:6**	850.5600	20.583	1.00
SM	**42:3**	855.6594	21.880	0.99
dPE	**34:2**	714.5093	13.647	0.98
Cer	**41:2**	678.6050	2.831	0.97
pPE	**38:5**	750.5450	13.090	0.96
TAG	**58:8**	948.8015	2.510	0.95
SM	**36:2**	773.5816	22.011	0.95
pPE	**40:7**	774.5451	12.965	0.95
TAG	**56:7**	922.7866	2.978	0.95
dPC	**34:0**	806.5823	21.158	0.94
TAG	**52:6**	870.7554	2.510	0.94
dPC	**36:6**	778.5388	19.573	0.94
SM	**34:1**	749.5820	21.968	0.93
dPE	**36:3**	740.5247	13.512	0.92
dPC	**36:5**	780.5518	19.975	0.91
Cer	**44:1**	722.6675	2.817	0.91
SM	**39:1**	773.6537	21.059	0.90
SM	**36:1**	775.5968	22.085	0.90
dPC	**34:3**	756.5552	19.901	0.90
dPE	**34:1**	716.5259	13.687	0.89
SM	**41:3**	841.6440	21.866	0.89
dPC	**34:1**	804.5748	21.145	0.88
SM	**34:1**	749.5720	22.139	0.87
SM	**38:0**	761.6439	21.047	0.87
dPE	**36:4**	738.5090	13.275	0.87
SM	**29:3**	673.5290	22.164	0.87
HexCer	**42:2**	854.6725	3.029	0.86
SM	**35:1**	717.5906	21.085	0.86
dPC	**38:5**	852.5750	20.720	0.86
dPC	**38:5**	808.5836	19.536	0.86
dPC	**32:2**	774.5295	21.109	0.86
dPC	**38:4**	810.6004	19.577	0.86
dPC	**38:6**	750.5295	21.341	0.85
Cer	**42:1**	694.6359	2.822	0.85